Cross-Layer MIMO Transceiver Optimization for Multimedia Streaming in Interference Networks

Fan Zhang, *StMIEEE*, Vincent K. N. Lau, *FIEEE*

Abstract—In this paper, we consider dynamic precoder/decorrelator optimization for multimedia streaming in MIMO interference networks. We propose a truly cross-layer framework in the sense that the optimization objective is the application level performance metrics for multimedia streaming, namely the *playback interruption* and *buffer overflow* probabilities. The optimization variables are the MIMO precoders/decorrelators at the transmitters and the receivers, which are adaptive to both the instantaneous channel condition and the playback queue length. The problem is a challenging multi-dimensional stochastic optimization problem and brute-force solution has exponential complexity. By exploiting the underlying timescale separation and special structure in the problem, we derive a closed-form approximation of the value function based on continuous time perturbation. Using this approximation, we propose a low complexity dynamic MIMO precoder/decorrelator control algorithm by solving an equivalent weighted MMSE problem. We also establish the technical conditions for asymptotic optimality of the low complexity control algorithm. Finally, the proposed scheme is compared with various baselines through simulations and it is shown that significant performance gain can be achieved.

I. INTRODUCTION

1) Background: There is a surge of interest in multimedia streaming in wireless systems and high quality real-time multimedia streaming applications pose great challenges to the design of the future wireless systems. In this paper, we consider multimedia streaming in MIMO interference networks where multiple BSs simultaneously deliver multimedia data to their associated mobile users over a shared wireless link. The performance of the interference network is fundamentally limited by the inter-cell interference from the cross links. There are many existing works on the interference mitigation for MIMO interference networks. In [1], [2], the authors show that interference alignment can achieve optimal degrees of freedom of a K-user interference network using infinite dimension time or frequency symbol extension. In [3], [4], the authors consider joint beamforming to minimize the sum mean squared error (MSE) or the transmit power of a multi-user MIMO system using optimization approaches. In [5], [6], the authors analyze the achievable rate region of a multi-antenna interference channel from a game-theoretic perspective and consider a distributed beamforming design using non-cooperative game. However, these solution frameworks are not *truly cross-layer design* [7], [8], in the sense that the optimization objectives are the physical layer metrics (e.g., throughput, SNR), which may

not be directly related to the application level performance metrics in multimedia streaming. Furthermore, the resulting control policy is adaptive to the channel state information (CSI) only, which exploits good transmission opportunities from the time-varying physical channels. However, for real-time multimedia streaming, dynamic control policy adaptive to the instantaneous queue length (QSI) is also very important because they give information about the *urgency* of the data flows.

Control policy adaptive to both the CSI and the QSI is very challenging because the associated optimization problem belongs to an infinite dimension stochastic optimization problem. A systematic approach is to formulate the problem into a Markov Decision Process (MDP) [9], [10]. In [11], [12], delay minimization using the MDP approach is considered. There are also a number of works [13], [14] that adopt the stochastic Lyapunov optimization technique for average delay minimization of wireless networks. However, these techniques cannot be easily used for multimedia streaming applications because average delay is not the end–to–end performance metric for multimedia streaming. For multimedia streaming applications, there is a playback buffer at the each mobile user and the *playback interruption probability* and the *buffer overflow probability* are the two important end–to–end performance metrics[1]. Playback interruption occurs when the playback buffer underflows and this is highly undesirable for the end user experience. On the other hand, due to the finite buffer size nature in practical systems, new packet arrivals will be dropped when playback buffer is full. This is also undesirable due to the wastage of wireless resource used to transmit these dropped packets. In [15], [16], the authors consider a fully dynamic power control and rate adaptation for video streaming over a wireless link using MDP. The optimality condition, namely the *Bellman equation*, is obtained and solved using conventional value iteration algorithm [9], [10]. However, the solution cannot be extended to deal with the multi-flow stochastic problem due to the curse of dimensionality. In our problem, there are K multimedia streaming flows in the system, and the queue dynamics of the K flows are complex-coupled together. This is because the *data rate* of each playback queue at the mobiles depends on the beamforming control actions of the other flows due to the mutual interference. As a result, brute-force value iteration or policy iteration [9], [10] will result in solutions with exponential complexity and they will not be

Fan Zhang and Vincent K. N. Lau are with Department of Electronic and Computer Engineering, Hong Kong University of Science and Technology, Hong Kong.

[1]Note that if we want to have good end-to-end performance for an application, we need to take the end-to-end performance metrics into the design considerations directly, instead of optimizing some intermediate performance metrics (such as weighted MMSE or sum rate).

viable in practice.

2) Our Contribution: In this paper, we consider a truly cross-layer optimization framework for real-time multimedia streaming applications in MIMO interference networks. Unlike many existing works on MIMO precoder/decorrelator optimization, the optimization objectives we consider, namely the *playback interruption* and *buffer overflow* probabilities, are directly related to the application level performance metrics. Furthermore, the optimization variables are the MIMO precoders/decorrelators which are adaptive to the instantaneous CSI and the instantaneous QSI at the playback buffers. The associated problem belongs to a K-dimensional stochastic optimization and brute-force solution [9], [10] has exponential complexity. By exploiting the special structure in the problem as well as the timescale separation between the slot duration and the interruption/overflow events, we obtained an *equivalent optimality condition* for the MDP in terms of a K-dimensional partial differential equation (PDE). The solution of the PDE is called the *value functions* and they capture the *dynamic urgency* of the K data flows. To deal with the challenge due to the queue coupling and the curse of dimensionality, we derive a closed-form approximate solution for the PDE using perturbation theory. Based on the derived approximate value function, the MIMO precoders/decorrelators are optimized by solving a per-stage weighted MMSE problem [17], where the instantaneous QSI affects the weights via the value function. While the per-stage problem is non-convex, we establish technical conditions for the asymptotic optimality of the proposed low complexity solution. Finally, we compare the proposed algorithm with various conventional beamforming schemes through simulations and show that significant performance gain can be achieved.

II. SYSTEM MODEL

In this section, we introduce the architecture of the multimedia streaming system in MIMO interference networks, the physical layer model as well as the playback queue model.

A. Architecture of the Multimedia Streaming System in MIMO Interference Networks

Fig. 1 shows a typical architecture of the multimedia streaming system in MIMO interference networks. The raw multimedia files are pre-compressed and saved in the storage devices in the multimedia streaming server (MSS). There are K mobile users streaming multimedia files from the MSS via a radio access network (RAN). Specifically, upon the request from the users, the MSS retrieves the pre-stored multimedia file and transmits it to the users over the RAN. Each mobile user k *consumes* the received multimedia packets at a constant playback rate μ_k. Furthermore, the RAN consists of K BSs, which are connected to the MSS via a high speed backhaul links. BS k sends information to user k. Each BS is equipped with $N_t \geq K$ antennas and each user is equipped with N_r antennas. All the K BSs share a common spectrum with bandwidth W Hz and hence, they potentially interfere with each other. In this paper, the time dimension is partitioned into decision slots indexed by t with slot duration τ. For example,
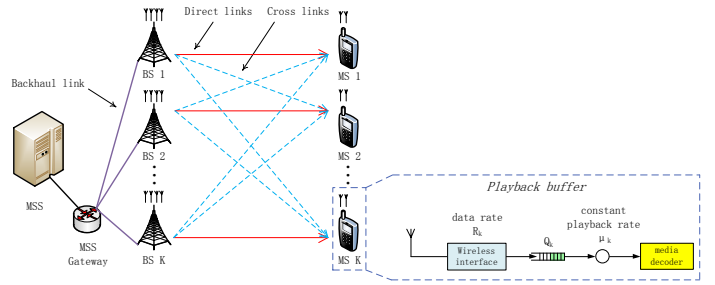

Fig. 1: Architecture of a multimedia system in MIMO interference network.

in LTE [18], the physical layer is organized into radio frames (corresponding to slot in our problem), and the generic radio frame has a time duration of 10 ms.

B. Physical Layer Model

The RAN and the K mobile users forms a MIMO interference network and the performance is limited by the inter-cell (cross channel) interference between the BSs. To deal with the interference issue, joint precoder/decorrelator optimization [19] is adopted at the BSs. Let $\mathbf{F}_k \in \mathbb{C}^{N_t \times d}$ be the transmit precoding matrix of BS k, where $d = \min\{N_t, N_r\}$ the number of data streams transmitted by each Tx-Rx pair[2]. Let $\mathbf{U}_k \in \mathbb{C}^{N_r \times d}$ be the decoding matrix of mobile user k. The received signal $\mathbf{y}_k \in \mathbb{C}^{d \times 1}$ at user k is given by

$$\mathbf{y}_k = \mathbf{U}_k^\dagger \big(\sqrt{L_{kk}} \mathbf{H}_{kk} \mathbf{F}_k \mathbf{s}_k + \sum_{j \neq k} \sqrt{L_{kj}} \mathbf{H}_{kj} \mathbf{F}_j \mathbf{s}_j + \mathbf{n}_k \big) \quad (1)$$

where $L_{kj} \in \mathbb{R}^+$ and $\mathbf{H}_{kj} \in \mathbb{C}^{N_r \times N_t}$ are the long-term channel path gain and short-term channel fading matrix from BS j to user k, respectively. $\mathbf{s}_k \in \mathbb{C}^{d \times 1}$ is the information symbol for BS k and we assume $\mathbb{E}[\mathbf{s}_k \mathbf{s}_k^\dagger] = \mathbf{I}$ [17]. In practical multimedia streaming applications, the information symbols are drawn from a finite alphabet constellation set of size $|\mathcal{S}|$, i.e., $\mathbf{s}_k \in \{\boldsymbol{\xi}_k^i\}_{i=1}^{|\mathcal{S}|}$ [20] for all k. $\mathbf{n}_k \sim \mathcal{CN}(0, \mathbf{I})$ is the i.i.d. complex AWGN noise vector. $(\cdot)^\dagger$ represents the conjugate transpose of a matrix. Denote the global CSI as $\mathbf{H} = \{\mathbf{H}_{kj} : \forall k, j\}$. We have the following assumption on $\mathbf{H}$:

Assumption 1 (Channel Fading Model): $\mathbf{H}_{kj}(t)$ remains constant within each decision slot and is i.i.d. over slots for all k, j. Specifically, each element of $\mathbf{H}_{kj}(t)$ follows a complex Gaussian distribution with zero mean and unit variance. Furthermore, $\mathbf{H}_{kj}(t)$ is independent w.r.t. k, j. The path gain L_{kj} remains constant for the duration of the communication session. ∎

For given CSI $\mathbf{H}$, precoding matrices $\mathbf{F} = \{\mathbf{F}_k : \forall k\}$ and decoding matrices $\mathbf{U}_k$, the achievable data rate for the k-th Tx-Rx pair (by treating interference as noise) is given by [21]

$$R_k(\mathbf{H}, \mathbf{F}, \mathbf{U}_k) = W \log_2 \det \Big(\mathbf{I} + \zeta L_{kk} \mathbf{U}_k^\dagger \mathbf{H}_{kk} \mathbf{F}_k \mathbf{F}_k^\dagger \mathbf{H}_{kk}^\dagger \mathbf{U}_k$$

[2]In this paper, we shall refer to BS as transmitter (Tx) and mobile users as receivers (Rx), and each BS and the associated mobile user pair as a Tx-Rx pair.
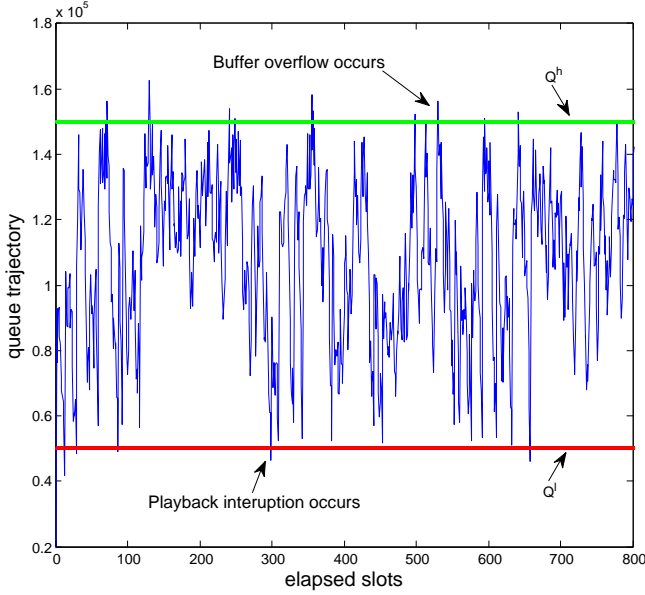
Fig. 2: Queue trajectory of the playback queue $Q_k(t)$ at the k-th mobile user. The system parameters are configured as in the simulations in Section VI.

$$\left(\sum_{j\neq k} L_{kj}\mathbf{U}_k^\dagger\mathbf{H}_{kj}\mathbf{F}_j\mathbf{F}_j^\dagger\mathbf{H}_{kj}^\dagger\mathbf{U}_k + \mathbf{I}\right)^{-1}\right) \quad (2)$$

where $\zeta \in (0,1]$ is a constant that is determined by the modulation and coding scheme (MCS) used in the system. For example, $\zeta = 0.5$ for QAM constellation at BER= 1% [21] and $\zeta = 1$ for capacity-achieving coding (in which, (2) corresponds to the instantaneous mutual information). In this paper, our derived results are based on $\zeta = 1$ for simplicity, which can be easily extended to other MCS cases.

Furthermore, the transmit power for BS k is given by [17]

$$P_k(\mathbf{F}_k) = \text{Tr}\left(\mathbf{F}_k\mathbf{F}_k^\dagger\right) \quad (3)$$

where $\text{Tr}(\cdot)$ represents the trace operator.

C. Playback Queue Dynamics at the Mobile Users

As shown in Fig. 1, each mobile user maintains a data queue for multimedia playback. Let $Q_k(t) \in \mathcal{Q}$ denote the QSI (number of bits) at the playback buffer of user k at the beginning of the t-th slot, where $\mathcal{Q} = [0,\infty)$ is the QSI state space. Let $\mathbf{Q}(t) = (Q_1(t),\ldots,Q_K(t)) \in \boldsymbol{\mathcal{Q}} \triangleq \mathcal{Q}^K$ denote the global QSI. The instantaneous arrivals of the k-th playback queue at slot t is given by $R_k(t)\tau$, which is controlled by the precoders $\mathbf{F}(t)$ and decorrelator $\mathbf{U}_k(t)$. The instantaneous departure of the k-th playback queue is given by $\mu_k\tau$, which is a constant and depends on the multimedia decoder at the end user. Hence, the queue dynamics for user k is given by

$$Q_k(t+1) = [Q_k(t) - \mu_k\tau]^+ + R_k(\mathbf{H}(t),\mathbf{F}(t),\mathbf{U}_k(t))\tau \quad (4)$$

where $[x]^+ = \max\{0,x\}$. It can be observed that the queue dynamics in the playback buffer is a Markovian queue with *controlled arrivals*.

Fig. 2 illustrates a trajectory of the playback queue $Q_k(t)$ for the k-th mobile user. The multimedia files are consumed by the user at a constant rate $\mu_k\tau$ during each slot. The system has to control the precoders $\mathbf{F}$ and decorrelators $\mathbf{U}$, so that $Q_k(t)$ will seldom go beyond certain level (i.e., the green line, which results in buffer overflow) or go below certain level (i.e., the red line, which results in playback interruption).

Remark 1 (Coupling Property of Queue Dynamics): The K queue dynamics in the MIMO interference network are coupled together due to the interference in (2). Specifically, the data rate R_k of each Tx-Rx pair k depends on the precoding matrices $\{\mathbf{F}_j : \forall j \neq k\}$ of all the other Tx-Rx pairs. Furthermore, the cross channel path gain $\{L_{kj} : \forall k,j, j \neq k\}$ measures the coupling intensity in the interference network. ∎

We have the following assumption on the interference network:

Assumption 2 (Weak Interference Network): For each Tx-Rx pair k, we assume the long-term cross channel path gains are much smaller than the direct channel path gain, i.e., $L_{kj} \ll L_{kk}, \forall j \neq k$. Furthermore, denote $L = \max\{L_{kj} : \forall k,j, k \neq j\}$ to be the largest (worst-case) cross channel path gain in the interference network. ∎

The assumption on the weak interference network can be justified in many applications. For example, due to the MAC filtering effect in some protocols, such as CSMA/CA [22], the interference in the cross channels cannot be too strong. The basic principle of the CSMA/CA is listen-before-talk [22], which is used to avoid collisions between simultaneous transmissions of the BSs in the neighboring cells. As a result, the MAC protocol determines the subset of the BSs in which the BSs can transmit data simultaneously without causing excessive interference. Suppose each BS uses a CSMA/CA MAC protocol with carrier sensing distance δ, then the worst-case path gain between two interfering BSs is given by[3] [23]: $L = G^r G^t \left(\frac{\lambda}{4\pi}\right)^2 \frac{1}{\delta^4}$, where G^r and G^t are the receive and transmit antenna gains respectively, and λ is the carrier wavelength. For instance, in IEEE 802.11g [24], the CSMA/CA sensing threshold is around -95 dBm, which corresponds to a sensing distance (i.e., δ) of around 188 m for the indoor environment. To support a 54 Mbps data rate, the receive sensitivity is around -75 dBm. Therefore, such a choice of carrier sensing distance corresponds to a worst-case cross channel path gain of at least 20 dB less than the direct channel path gain. We shall exploit this weak interference coupling property in Section IV to derive a closed-form approximate solution to the multi-dimensional MDP problem.

III. STOCHASTIC PRECODER AND DECORRELATOR CONTROL PROBLEM FORMULATION

In this section, we define the precoder and decorrelator control policy and formulate the stochastic control problem for multimedia streaming in the MIMO interference network.

---

[3]Here we adopt the Friis path loss model with exponent of 4 [23], which corresponds to the environment with obstructings in buildings. Note that the results of this paper can be extended easily for other path loss models.

A. MIMO Precoder and Decorrelator Control Policy

For notation convenience, we denote $\chi = (\mathbf{H}, \mathbf{Q})$ as the global system state. At the beginning of each decision slot, the controller determines the precoders $\mathbf{F} = \{\mathbf{F}_k : \forall k\}$ and decorrelators $\mathbf{U} = \{\mathbf{U}_k : \forall k\}$ to minimize the playback interruption and buffer overflow probabilities of the multimedia streaming applications based on the global system state χ according to the following stationary control policy:

Definition 1: (Stationary Precoder and Decorrelator Control Policy) A stationary precoder and decorrelator control policy Ω_k for Tx-Rx pair k is a mapping from the global system state χ to the precoding matrix of BS k and decoding matrices of user k. Specifically, we have $\Omega_k(\chi) = \{\mathbf{F}_k \in \mathbb{C}^{N_t \times d}, \mathbf{U}_k \in \mathbb{C}^{N_r \times d}\}$. Furthermore, let $\Omega = \{\Omega_k : \forall k\}$ denote the aggregation of the control policies for all the K BSs. ∎

Given a control policy Ω, the induced random process $\{\chi(t)\}$ is a controlled Markov chain with the following transition probability:

$$\Pr\left[\chi(t+1) \,\middle|\, \chi(t), \Omega(\chi(t))\right] \tag{5}$$
$$= \Pr\left[\mathbf{H}(t+1)\right] \Pr\left[\mathbf{Q}(t+1) \,\middle|\, \chi(t), \Omega(\chi(t))\right]$$
$$= \Pr\left[\mathbf{H}(t+1)\right] \prod_{k=1}^{K} \Pr\left[Q_k(t+1) \,\middle|\, Q_k(t), \mathbf{H}(t), \Omega(\chi(t))\right]$$

where $\Pr\left[Q_k(t+1) \,\middle|\, Q_k(t), \mathbf{H}(t), \Omega(\chi(t))\right]$ is the queue transition probability for the k-th Tx-Rx pair and is given by

$$\Pr\left[Q_k(t+1) \,\middle|\, Q_k(t), \mathbf{H}(t), \Omega(\chi(t))\right]$$
$$= \begin{cases} 1 & \text{if } Q_k(t+1) = [Q_k(t) - \mu_k\tau]^+ \\ & \qquad + R_k(\mathbf{H}(t), \mathbf{F}(t), \mathbf{U}_k(t))\tau \\ 0 & \text{otherwise} \end{cases} \tag{6}$$

Note that the last equality in (5) is due to the queue evolution equation in (4). Hence, $\{Q_k(t)\}$ is a controlled Markov chain and the next transition $Q_k(t+1)$ only depends on $Q_k(t)$, $\mathbf{H}(t)$, and $(\mathbf{F}, \mathbf{U}_k)$.

Furthermore, we have the following definition on the admissible control policy:

Definition 2 (Admissible Control Policy): A policy Ω is admissible if the following requirements are satisfied:

- Ω is a unichain policy, i.e., the controlled Markov chain $\{\chi(t)\}$ under Ω has a single recurrent class (and possibly some transient states) [10].
- The queueing system under Ω is stable in the sense that $\lim_{t\to\infty} \mathbb{E}^\Omega\left[\sum_{k=1}^K Q_k(t)\right] < \infty$, where $\mathbb{E}^\Omega$ means taking expectation w.r.t. the probability measure induced by the control policy Ω. ∎

B. Multimedia Streaming Performance and Cross-Layer Problem Formulation

The system performance of the multimedia system is characterized by the average transmit power of the BSs, playback interruption probability and buffer overflow probability of the mobile users.

Under an admissible control policy Ω, the average power cost of BS k starting from a given initial state $\chi(0)$ is given by

$$\overline{P}_k^\Omega((\chi(0))) = \limsup_{T\to\infty} \frac{1}{T} \sum_{t=0}^{T-1} \mathbb{E}^\Omega\left[P_k(\mathbf{F}_k(t))\right] \tag{7}$$

where $P_k(\mathbf{F}_k)$ is defined in (3). Similarly, under an admissible control policy Ω, the playback interruption probability and buffer overflow probability of user k are given by

$$\overline{I}_k^\Omega((\chi(0))) = \limsup_{T\to\infty} \frac{1}{T} \sum_{t=0}^{T-1} \mathbb{E}^\Omega\left[\mathbb{1}\left(Q_k(t) < Q^l\right)\right]$$
$$\approx \limsup_{T\to\infty} \frac{1}{T} \sum_{t=0}^{T-1} \mathbb{E}^\Omega\left[e^{-\eta[Q_k(t) - Q^l]^+}\right] \tag{8}$$

$$\overline{B}_k^\Omega((\chi(0))) = \limsup_{T\to\infty} \frac{1}{T} \sum_{t=0}^{T-1} \mathbb{E}^\Omega\left[\mathbb{1}\left(Q_k(t) > Q^h\right)\right]$$
$$\approx \limsup_{T\to\infty} \frac{1}{T} \sum_{t=0}^{T-1} \mathbb{E}^\Omega\left[e^{-\eta[Q^h - Q_k(t)]^+}\right] \tag{9}$$

where $Q^l > 0$ and $Q^h > 0$ are the target minimum and maximum playback buffer size at the mobile users, respectively, and we require $Q^h > Q^l$. Fig. 2 illustrates an example of the queue trajectory and the playback interruption/overflow events. During the playback interruption, the multimedia playback is frozen, which affects the end user experience. During the overflow event, the arrival packets are dropped and this causes wastage of the radio resource used to transmit the dropped packets. For technicality, we use $e^{-\eta[Q_k - Q^l]^+}$ and $e^{-\eta[Q^h - Q_k]^+}$ as a smooth approximation for the indicator functions in (8) and (9), where $\eta > 0$ is a parameter[4] of the smooth approximation. Fig. 3 and Fig. 4 illustrate the comparison of the actual and approximate playback interruption and buffer overflow per-stage costs. It can be observed that the approximate per-stage playback interruption (or buffer overflow) cost $e^{-\eta[Q_k - Q^l]^+}$ (or $e^{-\eta[Q^h - Q_k]^+}$) is very close to the actual per-stage cost $\mathbb{1}\left(Q_k < Q^l\right)$ (or $\mathbb{1}\left(Q_k > Q^h\right)$) for large values of η (e.g., $\eta \geq 10$).

We consider a truly cross-layer framework for the MIMO precoder/decorrelator optimization with the optimization objective to be the weighted sum of the average transmit power, the average playback interruption and the average buffer overflow probabilities of the multimedia streaming applications. This is formally stated below.

Problem 1: (Stochastic Precoder and Decorrelator Control Problem) For some positive constants $\boldsymbol{\gamma} = \{\gamma_k > 0 : \forall k\}$ and $\boldsymbol{\beta} = \{\beta_k > 0 : \forall k\}$, the stochastic precoder and decorrelator control problem is formulated as

$$\min_\Omega \quad L_{\boldsymbol{\gamma}, \boldsymbol{\beta}}^\Omega(\chi(0)) \tag{10}$$
$$= \sum_{k=1}^{K} \left(\overline{P}_k^\Omega((\chi(0))) + \gamma_k \overline{I}_k^\Omega((\chi(0))) + \beta_k \overline{B}_k^\Omega((\chi(0)))\right)$$

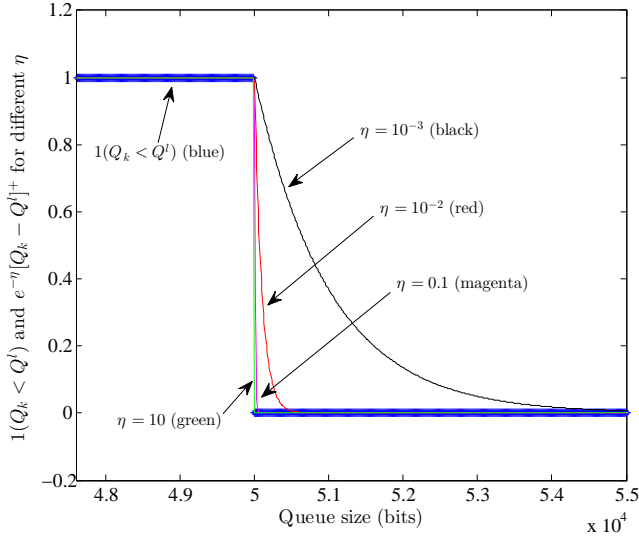[4]The approximation is asymptotically accurate as $\eta \to \infty$.

Fig. 3: Actual per-stage playback interruption cost $1(Q_k < Q^l)$ and the associated approximation $e^{-\eta[Q_k - Q^l]^+}$ for different values of η.
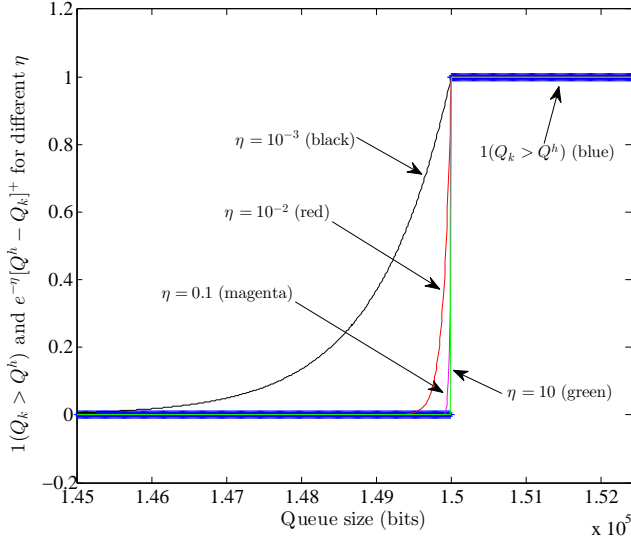

Fig. 4: Actual per-stage buffer overflow cost $1\left(Q_k > Q^h\right)$ and the associated approximation $e^{-\eta[Q^h - Q_k]^+}$ for different values of η.

$$= \limsup_{T \to \infty} \frac{1}{T} \sum_{t=0}^{T-1} \mathbb{E}^\Omega \left[c\left(\mathbf{Q}\left(t\right), \Omega\left(\boldsymbol{\chi}\left(t\right)\right)\right) \right]$$

where $\boldsymbol{\gamma}$ and $\boldsymbol{\beta}$ measures the relative importances[5] and tradeoffs of the playback interruption probability and buffer overflow probability. $c\left(\mathbf{Q}, \mathbf{F}\right) = \sum_{k=1}^K c_k\left(Q_k, \mathbf{F}_k\right)$ is the per-stage cost function with $c_k\left(Q_k, \mathbf{F}_k\right) = \mathrm{Tr}\left(\mathbf{F}_k \mathbf{F}_k^\dagger\right) + \gamma_k e^{-\eta[Q_k - Q^l]^+} + \beta_k e^{-\eta[Q^h - Q_k]^+}$. ∎

Note that the two technical conditions in Definition 2 on the admissible policy ensure that there is a unique solution to Problem 1. Furthermore, Problem 1 is an infinite horizon

average cost MDP, which is well-known to be a very difficult problem [25]. In the next subsection, by exploiting the special structure in our problem, we derive an equivalent optimality equation to simplify the MDP problem.

C. Optimality Conditions and Approximate Optimality Equation

While the MDP in Problem 1 is difficult in general, we utilize the i.i.d. assumption of the CSI to derive an *equivalent optimality equation* as summarized below.

Theorem 1 (Sufficient Conditions for Optimality): For any given $\boldsymbol{\gamma}$ and $\boldsymbol{\beta}$, assume there exists a $(\theta^*, \{V^*(\mathbf{Q})\})$ that solves the following *equivalent optimality equation*:

$$\theta^*\tau + V^*\left(\mathbf{Q}\right), \qquad \forall \mathbf{Q} \in \boldsymbol{\mathcal{Q}} \qquad (11)$$
$$= \mathbb{E}\left[\min_{\mathbf{F},\mathbf{U}} \left[c\left(\mathbf{Q}, \mathbf{F}\right)\tau + \sum_{\mathbf{Q}'} \Pr\left[\mathbf{Q}'\big|\boldsymbol{\chi}, \mathbf{F}, \mathbf{U}\right] V^*\left(\mathbf{Q}'\right) \right] \bigg| \mathbf{Q} \right]$$

Furthermore, for all admissible control policy Ω and initial queue state $\mathbf{Q}(0)$, V^* satisfies the following *transversality condition*:

$$\lim_{T \to \infty} \frac{1}{T} \mathbb{E}^\Omega \left[V^*\left(\mathbf{Q}\left(T\right)\right) | \mathbf{Q}\left(0\right) \right] = 0 \qquad (12)$$

Then, $\theta^* = \min_\Omega L_{\boldsymbol{\gamma}, \boldsymbol{\beta}}^\Omega\left(\boldsymbol{\chi}\left(0\right)\right)$ is the optimal average cost for any initial state $\boldsymbol{\chi}(0)$ and $V^*(\mathbf{Q})$ is called the *value function*. If $(\mathbf{F}^*, \mathbf{U}^*)$ attains the minimum of the R.H.S. in (11) for given $\boldsymbol{\chi}$, then the optimal control policy of Problem 1 is given by $\Omega^*\left(\boldsymbol{\chi}\right) = (\mathbf{F}^*, \mathbf{U}^*)$. ∎

Proof: please refer to Appendix A. ∎

Solving (11) is a difficult problem because it corresponds to solving a series of fixed point equations w.r.t. $(\theta^*, \{V^*(\mathbf{Q})\})$ which involves exponentially many equations and unknowns. This explains why standard solutions such as value iteration and policy iteration [9], [10] have exponential complexity w.r.t. K. Instead of solving (11) directly, we exploit the timescale separation property between the slot duration τ and the interruption/overflow events and establish an approximate optimality equation to further simplify our problem.

Corollary 1 (Approximate Optimality Equation): For any given $\boldsymbol{\gamma}$ and $\boldsymbol{\beta}$, if

- there is a unique $(\theta^*, \{V^*(\mathbf{Q})\})$ that satisfies the optimality equation and transversality condition in Theorem 1.
- there exist θ and $V(\mathbf{Q})$ of class[6] $\mathcal{C}^2(\mathbb{R}_+^K)$ that solve the following *approximate optimality equation*:

$$\theta = \mathbb{E}\left[\min_{\mathbf{F},\mathbf{U}} \left[c\left(\mathbf{Q}, \mathbf{F}\right) + \qquad \forall \mathbf{Q} \in \boldsymbol{\mathcal{Q}} \quad (13) \right.\right.$$
$$\left.\left. \sum_{k=1}^K \frac{\partial V\left(\mathbf{Q}\right)}{\partial Q_k}\left(R_k\left(\mathbf{H}, \mathbf{F}, \mathbf{U}_k\right) - \mu_k\right) \right] \bigg| \mathbf{Q} \right]$$

Furthermore, for all admissible control policy Ω and initial queue state $\mathbf{Q}(0)$, the transversality condition in (12) is satisfied for V.

then, we have

$$\theta^* = \theta + o(1), \quad V^*(\mathbf{Q}) = V(\mathbf{Q}) + o(1), \quad \forall \mathbf{Q} \in \mathcal{Q} \quad (14)$$

where the error term $o(1)$ asymptotically goes to zero for sufficiently small slot duration τ. ∎

Proof: Please refer to Appendix B. ∎

Corollary 1 states that the difference between $(\theta, \{V(\mathbf{Q})\})$ obtained in (14) and $(\theta^*, \{V^*(\mathbf{Q})\})$ in (11) is asymptotically small w.r.t. the slot duration τ. Therefore, we can focus on solving the approximate optimality equation in (14), which is a simpler problem than solving the original optimality equation in (11).

IV. Closed-Form Approximate Value Function based on Calculus Approach

In this section, we adopt a calculus approach to obtain a closed-form approximation of the value function. Specifically, we shall exploit the weak interference property and utilize the perturbation theory to obtain the approximate value function.

A. Multi-dimensional PDE

We first have the following theorem for solving the approximate optimality equation in (14):

Theorem 2: (Calculus Approach on Solving the Approximate Optimality Equation) Assume there exist c^∞ and $J(\mathbf{Q}; L)$ of class $\mathcal{C}^2(\mathbb{R}_+^K)$ that satisfy

- the following multi-dimensional PDE:

$$\mathbb{E}\left[\min_{\mathbf{F}, \mathbf{U}} \left[c(\mathbf{Q}, \mathbf{F}) + \right. \right. \qquad \mathbf{Q} \in \mathbb{R}_+^K \quad (15)$$

$$\left. \left. \sum_{k=1}^{K} \frac{\partial J(\mathbf{Q}; L)}{\partial Q_k} \left(R_k(\mathbf{H}, \mathbf{F}, \mathbf{U}_k) - \mu_k \right) \right] \middle| \mathbf{Q} \right] - c^\infty = 0$$

with boundary condition $J(Q_1^\star, \ldots, Q_K^\star; L) = 0$, where $Q_k^\star$ $(\forall k)$ are some given constant queue values.
- $\frac{\partial J(\mathbf{Q}; L)}{\partial Q_k} > 0$ for sufficiently large Q_k for all k.
- $J(\mathbf{Q}; L) = \mathcal{O}\left(\sum_{k=1}^{K} Q_k \right)$.

Then, we have

$$\theta^* = c^\infty + o(1), \quad V^*(\mathbf{Q}) = J(\mathbf{Q}; L) + o(1), \quad \forall \mathbf{Q} \in \mathcal{Q} \quad (16)$$

∎

Proof: please refer to Appendix C. ∎

As a result, solving the approximate optimality equation in (14) is transformed into a calculus problem of solving the PDE in (15). However, the PDE is still a K-dimensional non-linear PDE, which is in general very challenging. To obtain a closed-form approximation of $V^*(\mathbf{Q})$, we apply perturbation analysis to a base PDE as shown in the next subsection.

B. Perturbation Approximation of $J(\mathbf{Q}; L)$

The solution of the multi-dimensions PDE in (15) depends on the worst-case cross channel path gain L and hence, the K-dimensional PDE can be regarded as a perturbation of a base PDE defined below.

Definition 3 (Base PDE): A base PDE is the PDE in (15) with $L = 0$. ∎

We then study the base PDE and use $J(\mathbf{Q}; 0)$ to obtain a closed-form approximation of $J(\mathbf{Q}; L)$. We have the following lemma summarizing the decomposable structure of c^∞ and $J(\mathbf{Q}; 0)$:

Lemma 1 (Decomposable Structure of c^∞ and $J(\mathbf{Q}; 0)$): If[7] $e^{\eta(Q^l - Q^h)} < \frac{\gamma_k}{\beta_k} < e^{\eta(Q^h - Q^l)}$ and $\beta_k > c_k^\infty$, then c^∞ and $J(\mathbf{Q}; 0)$ in the base PDE has the following decomposable structure:

$$c^\infty = \sum_{k=1}^{K} c_k^\infty, \quad J(\mathbf{Q}; 0) = \sum_{k=1}^{K} J_k(Q_k) \quad (17)$$

where c_k^∞ is given by (46) and $J_k'(Q_k)$ is determined[8] by the fixed point equation in (47) in Appendix D. Furthermore, we have the following asymptotic property of $J_k(Q_k)$:

$$J_k(Q_k) = C_k Q_k, \quad \text{as } Q_k \to \infty \quad (18)$$

where $C_k = \frac{\beta_k - c_k^\infty}{\mu_k}$ is a positive constant. ∎

Proof: Please refer to Appendix D. ∎

Next, we approximate $J(\mathbf{Q}; L)$ as a perturbation of $J(\mathbf{Q}; 0)$. Using perturbation analysis, we establish the following theorem on the approximation of $J(\mathbf{Q}; L)$.

Theorem 3 (Perturbation Approximation of $J(\mathbf{Q}; L)$): $J(\mathbf{Q}; L)$ can be approximated by $J(\mathbf{Q}; 0)$ and the first order perturbation term is given by

$$J(\mathbf{Q}; L) = \sum_{k=1}^{K} J_k(Q_k) - \sum_{k=1}^{K} \sum_{j \neq k} L_{kj} h_{kj}(Q_k, Q_j) + \mathcal{O}(L^2) \quad (19)$$

where $h_{kj}(Q_k, Q_j) = o(1)$, if either $Q_k > Q_k^\star$ or $Q_j > Q_j^\star$, and $h_{kj}(Q_k, Q_j) = E_{kj}(Q_k - Q_k^\star) + E_{jk}(Q_j - Q_j^\star) + o(Q_k) + o(Q_j)$ $(k \neq j)$, otherwise. $Q_k^\star = \frac{Q^l + Q^h}{2} + \frac{1}{2\eta} \ln \frac{\gamma_k}{\beta_k} \in (Q^l, Q^h)$ and $E_{kj} = \frac{\ln 2(c_k^1 D_k + c_k^2)(c_j^1 D_j + c_j^2)}{2dW(\mu_k - c_k^1 \ln(-D_k) - c_k^3)}$ is a constant (c_k^1, c_k^2, c_k^3 and D_k are given in (52)–(55) in Appendix E.) ∎

Proof: Please refer to Appendix E. ∎

Finally, based on Theorem 2 and Theorem 3, we propose the following closed-form approximation of the relative value function:

$$V^*(\mathbf{Q}) \approx \widetilde{V}(\mathbf{Q}) \triangleq \sum_{k=1}^{K} J_k(Q_k) - \sum_{k=1}^{K} \sum_{j \neq k} L_{kj} \widetilde{h}_{kj}(Q_k, Q_j) \quad (20)$$

where $\widetilde{h}_{kj}(Q_k, Q_j) = 0$, if either $Q_k > Q_k^\star$ or $Q_j > Q_j^\star$, and $\widetilde{h}_{kj}(Q_k, Q_j) = E_{kj}(Q_k - Q_k^\star) + E_{jk}(Q_j - Q_j^\star)$, otherwise.

Furthermore, based on Lemma 1 and (20), we have $\frac{\partial J(\mathbf{Q}; L)}{\partial Q_k} > 0$ for sufficiently large Q_k $(\forall k)$, and $\widetilde{V}(\mathbf{Q}) =$

---

[7]These conditions on the weights $\boldsymbol{\gamma}$ and $\boldsymbol{\beta}$ are imposed to make sure there is a solution for (15) in Theorem 2. Qualitatively, if β_k is too small, the power cost in Problem 1 will dominate and the user k will not be served at all (they will be allocated zero power). These conditions are used to avoid such uninteresting degenerated case.

[8]The optimal control policy by solving (15) only requires the partial derivatives of the value functions $\{ \frac{\partial J(\mathbf{Q}; L)}{\partial Q_k} : \forall k \}$, so we can focus on deriving $J_k'(Q_k)$ in the based PDE.
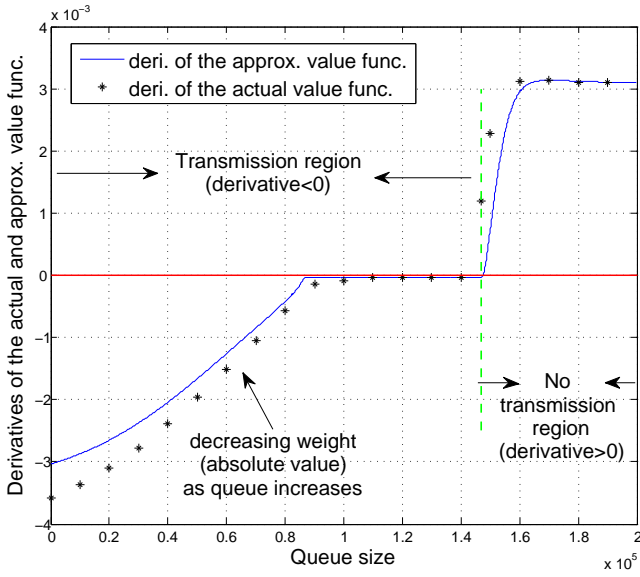
Fig. 5: Derivatives of the actual value function $\frac{\partial V^*(\mathbf{Q})}{\partial Q_k}$ and approximate value function $\frac{\partial \widetilde{V}(\mathbf{Q})}{\partial Q_k}$ versus the playback queue Q_k with $\mathbf{Q} = (Q_1, 50K, 100K, 150K)$ and $\eta = 50$. The system parameters are configured as in the simulations in Section VI.

$\mathcal{O}\left(\sum_{k=1}^{K} Q_k\right)$. Based on Theorem 2 and Theorem 3, the approximation error between the optimal value function $V^*(\mathbf{Q})$ in Theorem 1 and the closed-form approximate value function $\widetilde{V}(\mathbf{Q})$ in (20) is $\mathcal{O}(L) + o(1)$. In other words, the error terms are asymptotically small w.r.t. the worst-case cross channel path gain[9] and the slot duration. Fig. 5 illustrates the comparison of the derivatives of the actual (optimal) value function and the approximate value function. In the next section, we derive a low complexity control policy using the closed-form approximate value function in (20).

V. LOW COMPLEXITY MIMO PRECODERS/DECORRELATORS BASED ON WMMSE

In this section, we use the closed-form approximate value function in (20) to capture the urgency information of the data flows and to obtain low complexity dynamic precoder and decorrelator control. We first show that minimizing the R.H.S. of the Bellman equation using the closed-form approximate value function is equivalent to solving a collection of per-stage control problems. We further transform the per-stage problem into an equivalent weighted sum-MSE minimization problem and obtain a low complexity dynamic precoder and decorrelator control algorithm by solving this problem.

A. Equivalent Per-Stage Control Problem

Using the approximate value function in (20) and Corollary 1, the per-stage control problem (for each state realization χ)

---

[9]Based on the Wi-Fi CSMA/CA example in Section II-C, L is very small and hence, the first order approximation in (20) is quite accurate.

is given by[10]

$$\min_{\mathbf{F}, \mathbf{U}} \sum_{k=1}^{K} \left(\text{Tr}\left(\mathbf{F}_k \mathbf{F}_k^{\dagger}\right) + \frac{\partial \widetilde{V}(\mathbf{Q})}{\partial Q_k} R_k\left(\mathbf{H}, \mathbf{F}, \mathbf{U}_k\right) \right) \quad (21)$$

Note that the weights $\left\{\frac{\partial \widetilde{V}(\mathbf{Q})}{\partial Q_k} : \forall k\right\}$ in the above per-stage control problem is determined by the instantaneous QSI. Fig. 5 illustrates $\frac{\partial \widetilde{V}(\mathbf{Q})}{\partial Q_k}$ versus Q_k. When Q_k is large, $-\frac{\partial \widetilde{V}(\mathbf{Q})}{\partial Q_k}$ is small and hence, the priority of the k-th flow is reduced. This is reasonable because when Q_k in the playback buffer of user k is large, the k-th flow can withstand intermittent fading or reduction in the instantaneous arrivals for some time before playback interruption occurs.

For given precoding matrices $\mathbf{F}$ and state realization χ, the optimal decoding matrices of the mobile users $\mathbf{U}^*(\mathbf{F}) = \{\mathbf{U}_k^*(\mathbf{F}) : \forall k\}$ are given by the MMSE receiver [17]:

$$\mathbf{U}_k^*(\mathbf{F}) = \mathbf{J}_k^{-1}(\mathbf{F}) L_{kk} \mathbf{H}_{kk} \mathbf{F}_k, \quad \forall k \quad (22)$$

where $\mathbf{J}_k(\mathbf{F}) = \sum_{j=1}^{K} L_{kj} \mathbf{H}_{kj} \mathbf{F}_j \mathbf{F}_j^{\dagger} \mathbf{H}_{kj}^{\dagger} + \mathbf{I}$ is the downlink signal plus noise covariance matrix. Using the MMSE receiver in (22), the per-stage control problem in (24) can be further transformed into the following equivalent form:

$$\min_{\mathbf{F}} \sum_{k=1}^{K} \left(\text{Tr}\left(\mathbf{F}_k \mathbf{F}_k^{\dagger}\right) + \frac{\partial \widetilde{V}(\mathbf{Q})}{\partial Q_k} R_k\left(\mathbf{H}, \mathbf{F}, \mathbf{U}_k^*(\mathbf{F})\right) \right) \quad (23)$$

where $R_k\left(\mathbf{H}, \mathbf{F}, \mathbf{U}_k^*(\mathbf{F})\right) = W \log_2 \det\left(\mathbf{I} + L_{kk} \mathbf{H}_{kk} \mathbf{F}_k \mathbf{F}_k^{\dagger} \mathbf{H}_{kk}^{\dagger}\left(\sum_{j \neq k} L_{kj} \mathbf{H}_{kj} \mathbf{F}_j \mathbf{F}_j^{\dagger} \mathbf{H}_{kj}^{\dagger} + \mathbf{I}\right)^{-1}\right)$.

Remark 2 (Interpretation of (23)): The precoding matrices obtained by solving (23) is adaptive to both the CSI and the QSI. Furthermore, for sufficiently large Q_k, $\frac{\partial \widetilde{V}(\mathbf{Q})}{\partial Q_k}$ is positive, which results in the associated optimal precoding matrices[11] to be $\mathbf{0}$. Therefore, for given QSI realization $\mathbf{Q}$, we can focus on the MIMO precoder/decorrelator design for the set of users $\mathcal{I}_k^{\mathbf{Q}} = \left\{k : \frac{\partial \widetilde{V}(\mathbf{Q})}{\partial Q_k} < 0\right\}$, while the precoders/decorrelators for the other users ($k \notin \mathcal{I}_k^{\mathbf{Q}}$) are set to be $\mathbf{0}$. ∎

B. Low Complexity MIMO Precoders/Decorrelators Solution

The per-stage problem in (23) can be further transformed into the following weighted sum-MSE minimization problem [17]:

Problem 2 (Weighted Sum-MSE Minimization Problem):

$$\min_{\mathbf{F}, \mathbf{Z}, \mathbf{K}} \sum_{k \in \mathcal{I}_k^{\mathbf{Q}}} \left(\text{Tr}(\mathbf{F}_k \mathbf{F}_k^{\dagger}) - \frac{\partial \widetilde{V}(\mathbf{Q})}{\partial Q_k} \frac{W}{\ln 2} \right.$$
$$\left. \left(\text{Tr}\left(\mathbf{Z}_k \mathbf{E}_k(\mathbf{F}, \mathbf{K})\right) - \ln \det \mathbf{Z}_k\right) \right) \quad (24)$$

where we denote $\mathbf{Z} = \left\{\mathbf{Z}_k : k \in \mathcal{I}_k^{\mathbf{Q}}\right\}$ and $\mathbf{Z}_k \succeq 0$ is a weight for user k, $\mathbf{K} = \left\{\mathbf{K}_k : k \in \mathcal{I}_k^{\mathbf{Q}}\right\}$ and $\mathbf{E}_k$ is the MSE given

---

[10]From (20), $\frac{\partial \widetilde{V}(\mathbf{Q})}{\partial Q_k} = J_k'(Q_k) - \sum_{j \neq k} \left(L_{kj} \widetilde{h}_{kj}'(Q_k, Q_j) + L_{jk} \widetilde{h}_{jk}'(Q_k, Q_j)\right)$, where $\widetilde{h}_{kj}'(Q_k, Q_j) = 0$, if either $Q_k > Q_k^\star$ or $Q_j > Q_j^\star$, and $\widetilde{h}_{kj}'(Q_k, Q_j) = E_{kj}$, otherwise.

[11]Please refer to Lemma 6 in Appendix C for the detailed proof.

by

$$\mathbf{E}_k\left(\mathbf{F},\mathbf{K}\right) = \left(\mathbf{I} - \sqrt{L_{kk}}\mathbf{K}_k^\dagger\mathbf{H}_{kk}\mathbf{F}_k\right)\left(\mathbf{I} - \sqrt{L_{kk}}\mathbf{K}_k^\dagger\mathbf{H}_{kk}\mathbf{F}_k\right)^\dagger$$
$$+ \sum_{\substack{j \neq k \\ j \in \mathcal{I}_k^\mathbf{Q}}} L_{kj}\mathbf{K}_k^\dagger\mathbf{H}_{kj}\mathbf{F}_j\mathbf{F}_j^\dagger\mathbf{H}_{kj}^\dagger\mathbf{K}_k + \mathbf{K}_k^\dagger\mathbf{K}_k \qquad (25)$$

■

Lemma 2: (Relationship Between the Problems in (23) and (24)) The problem in (24) is equivalent to the problem in (23), i.e., the global optimal solution $\mathbf{F}^*$ for the two problems are identical. ■

Proof: The proof follows similar approach as in [17, Theorem 1]. Details are omitted due to page limit. ■

The sum-MSE cost function in (24) is not jointly convex in all the optimization variables $\{\mathbf{F}_k, \mathbf{Z}_k, \mathbf{K}_k : k \in \mathcal{I}_k^\mathbf{Q}\}$, but it is convex in each of $\{\mathbf{F}_k, \mathbf{Z}_k, \mathbf{K}_k : k \in \mathcal{I}_k^\mathbf{Q}\}$ while holding the others fixed. Therefore, we propose to use an alternating iterative algorithm to solve the WMMSE problem in Problem 2. In particular, we minimize the sum-MSE cost function by sequentially updating one of $\{\mathbf{F}_k, \mathbf{Z}_k, \mathbf{K}_k : k \in \mathcal{I}_k^\mathbf{Q}\}$ and fixing the others. The precoder and decorrelator control algorithm based on WMMSE is given as follows:

Algorithm 1: (Low Complexity Dynamic Precoder and Decorrelator Control:)

- **Step 1 [Initialization]:** Set $n = 0$ and each BS k initializes $\mathbf{F}_k(0)$.
- **Step 2 [Message Passing between BSs and Mobile Users]:** Each user k broadcasts its local QSI to the K BSs, and then each BS k calculates $\left\{\frac{\partial \widetilde{V}(\mathbf{Q})}{\partial Q_k} : \forall k\right\}$ locally. If $\frac{\partial \widetilde{V}(\mathbf{Q})}{\partial Q_k} < 0$, the k-th Tx-Rx pair will participate in the precoder/decorrelator iterative calculations in the current slot. Otherwise, the associated precoder/decorrelator are set to be $\mathbf{0}$.
- **Step 3 [Update on K and Z]:** Each BS k ($k \in \mathcal{I}_k^\mathbf{Q}$) informs the associated mobile user k of the updated $\mathbf{F}_k$. Each user k ($k \in \mathcal{I}_k^\mathbf{Q}$) locally estimates the downlink signal plus noise covariance matrix $\mathbf{J}_k(\mathbf{F})$, and updates $\mathbf{K}_k$ and $\mathbf{Z}_k$ according to the following equations:
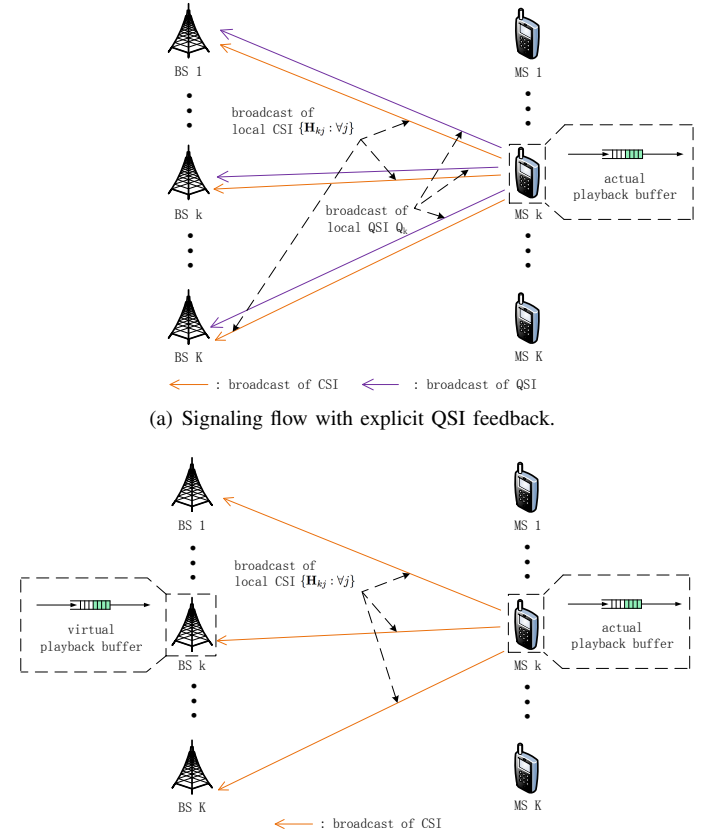
$$\mathbf{K}_k(n+1) = \mathbf{J}_k^{-1}(\mathbf{F}(n))\sqrt{L_{kk}}\mathbf{H}_{kk}\mathbf{F}_k(n) \qquad (26)$$

$$\mathbf{Z}_k(n+1) = \left(\mathbf{I} - \mathbf{K}_k^\dagger(n)\sqrt{L_{kk}}\mathbf{H}_{kk}\mathbf{F}_k(n)\right)^{-1} \qquad (27)$$

- **Step 4 [Update on F]:** Each user k ($k \in \mathcal{I}_k^\mathbf{Q}$) feeds back the updated $\mathbf{K}_k, \mathbf{Z}_k$ to each associated BS k. Each BS k locally updates $\mathbf{F}_k$ according to the following equations:

$$\mathbf{F}_k(n+1) = -\frac{\partial \widetilde{V}(\mathbf{Q})}{\partial Q_k}\frac{W}{\ln 2}\Big(\sum_j -\frac{\partial \widetilde{V}(\mathbf{Q})}{\partial Q_j}\frac{W}{\ln 2}L_{jk}$$

$$\mathbf{H}_{jk}^\dagger\mathbf{K}_j(n+1)\mathbf{Z}_j(n+1)\mathbf{K}_j^\dagger(n+1)\mathbf{H}_{jk} + \mathbf{I}\Big)^{-1}$$

$$\sqrt{L_{kk}}\mathbf{H}_{kk}^\dagger\mathbf{K}_k(n+1)\mathbf{Z}_k(n+1) \qquad (28)$$

- **Step 5 [Termination]:** Set $n = n + 1$ and go to Step 3 until a certain termination condition is satisfied. ■

(a) Signaling flow with explicit QSI feedback.

(b) Signaling flow with virtual queue at each BS and without explicit QSI feedback.

Fig. 6: Illustrations of the signaling flow of Algorithm 1 and the virtual queue at the BS for each Tx-Rx pair k.

Lemma 3 (Convergence Property of Algorithm 1): Any limiting point $\{\mathbf{F}(\infty), \mathbf{Z}(\infty), \mathbf{K}(\infty)\}$ of Algorithm 1 is a stationary point of Problem 2, and $\mathbf{F}(\infty)$, $\mathbf{K}(\infty)$ (corresponding to $\mathbf{U}^*$ in (22) according to (26)) is a stationary point of the problem in (23). Furthermore, Algorithm 1 converges to the unique global optimal point of the problem in (23) for sufficiently small L. ■

Proof: Please refer to Appendix F. ■

C. Summary of the Dynamic MIMO Precoder/Decorrelator Control and Performance Analysis

Fig. 6 illustrates the signaling flow of Algorithm 1. We have the following remark discussing the signaling overhead of the algorithm:

Remark 3 (Signaling Overhead of Algorithm 1): Our proposed algorithm has very low signaling overhead. To implement Algorithm 1, all the BSs need to know the CSI matrices of the interference channels, and the QSI at the playback buffers of all the mobile users. Specifically,

- **CSI Signaling:** The knowledge of the CSI matrices at all the K BSs can be achieved by each mobile user k broadcasting the local CSI measurements $\{\mathbf{H}_{kj} : \forall j\}$ to the K BSs as illustrated in Fig. 6. This CSI signaling requirement is the same as the conventional interference mitigation schemes in cooperative/coordinate MIMO [17], [26].

- **QSI Signaling:** Besides the CSI signaling, an additional signaling requirement is the QSI. This can be achieved by each user k broadcasting Q_k to all the K BSs as illustrated in Fig. 6(a). Since Q_k is a scalar, the additional signaling cost is negligible compared with the CSI signaling (which is a matrix feedback), and such scalar signaling can be easily supported by the existing LTE measurement messages [18]. Furthermore, for constant playback rate at each mobile user, there is no need to explicitly feedback Q_k to the BSs, because each BS k can keep track of the transmit bits to the associated MS k. Therefore, each BS k can maintain a virtual queue process as shown in Fig. 6(b), which has the same queue dynamics as the playback buffer at the mobile user. ■

We have the following remark discussing the complexity of the Algorithm 1:

Remark 4 (Complexity Analysis of Algorithm 1): The computational complexity of Algorithm 1 is very low. Specifically, the complexity comes from computing the approximate value function in (20) and the precoding matrices in Algorithm 1. The complexity of computing the closed-form approximate value function is very low compared with conventional value iteration methods [10]. Computing the precoding matrices in Algorithm 1 is fast since each mobile user only needs to do twice matrix inversions (as in (26) and (27)) and each BS needs to do one matrix inversions (as in (28)) based on local information at each time slot. Table. I illustrates the comparison of the MATLAB computational time of the proposed solution, the baselines and the brute-force value iteration algorithm [10]. ■

Finally, we analyze the performance gap between the optimal solution (by solving (11)) and the low complexity solution in Algorithm 1. Let $\widetilde{\Omega}$ represent the precoder and decorrelator control policy in Algorithm 1 and $\widetilde{\theta} = \limsup_{T \to \infty} \frac{1}{T} \sum_{t=0}^{T-1} \mathbb{E}^{\widetilde{\Omega}} \left[c \left(\mathbf{Q}(t), \Omega(\boldsymbol{\chi}(t)) \right) \right]$ be the associated average performance. The performance gap between $\widetilde{\theta}$ and the optimal average cost θ^* in (11) is established in the following theorem:

Theorem 4 (Performance Gap between $\widetilde{\theta}$ and θ^*): The performance gap between $\widetilde{\theta}$ and θ^* is given by

$$\widetilde{\theta} - \theta^* = \mathcal{O}(L) + o(1), \qquad \text{as } L \to 0, \tau \to 0 \tag{29}$$

■

Proof: Please refer to Appendix G. ■

Theorem 4 suggests that $\widetilde{\theta} \to \theta^*$, as $L \to 0$ and $\tau \to 0$. In other words, the proposed precoder and decorrelator control algorithm in Algorithm 1 is asymptotically optimal as $L \to 0$ and $\tau \to 0$.

VI. SIMULATIONS

In this section, we compare the performance of the proposed precoder and decorrelator control scheme for multimedia streaming in Algorithm 1 with the following three baselines using numerical simulations:

- **Baseline 1, Zero-Forcing Precoding (ZFP) [26]:** The K BSs adopt zero-forcing precoding matrix and fixed power transmission at each time slot. The precoding matrix of
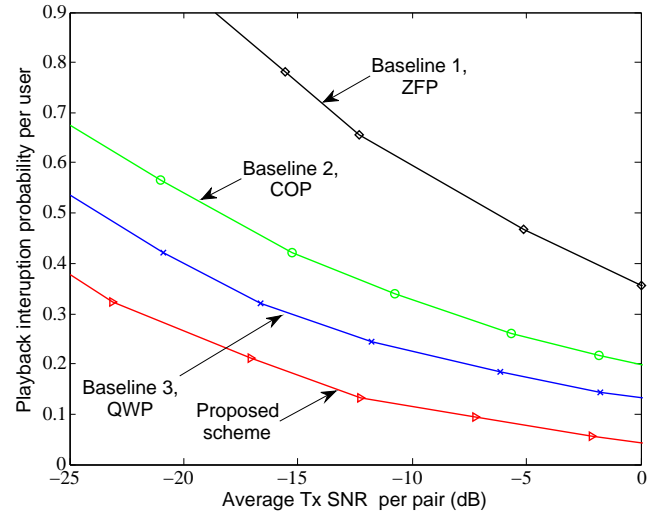

Fig. 7: Playback interruption probability per user versus average Tx SNR per pair, with $K = 5$, $N_t = 5$ and $N_r = 2$.
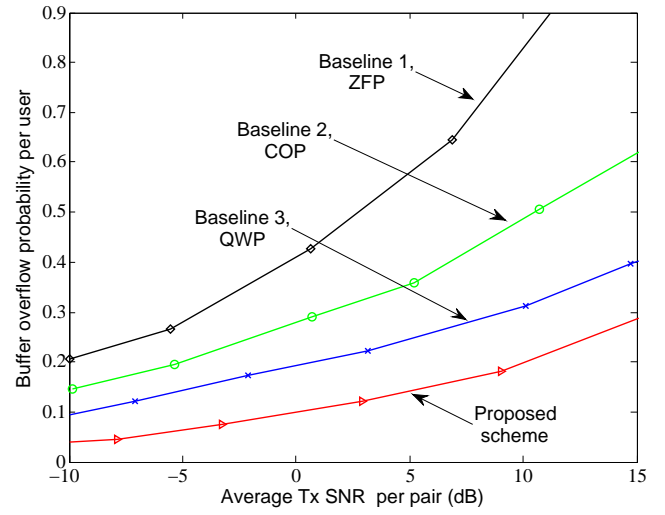

Fig. 8: Buffer overflow probability per user versus average Tx SNR per pair, with $K = 5$, $N_t = 5$ and $N_r = 2$.

BS k is obtained by projection of $\mathbf{H}_{kk}$ on the orthogonal complement of the subspace span $\left([\mathbf{H}_{jk}]_{j \neq k} \right)$.

- **Baseline 2, CSI-Only Precoding (COP) [17]:** The precoding matrix of each BS is obtained by solving the following problem at each time slot: $\min_{\mathbf{F}, \mathbf{U}} \sum_{k=1}^{K} \left(\text{Tr} \left(\mathbf{F}_k \mathbf{F}_k^\dagger \right) - \alpha R_k \left(\mathbf{H}, \mathbf{F}, \mathbf{U}_k \right) \right)$ for all k, where α is used to adjust the tradeoff between the transmit power and the data rate. The optimal CSI-only precoding control is only adaptive to CSI.

- **Baseline 3, Queue-Weighted Precoding (QWP) [13]:** The precoding matrix of each BS is obtained by solving the following problem at each time slot: $\min_{\mathbf{F}, \mathbf{U}} \sum_{k=1}^{K} \left(\text{Tr} \left(\mathbf{F}_k \mathbf{F}_k^\dagger \right) - \alpha [Q^h - Q_k]^+ \right.$ $\left. \times R_k \left(\mathbf{H}, \mathbf{F}, \mathbf{U}_k \right) \right)$ for all k. The optimal queue-weighted precoding control is adaptive to CSI and QSI.

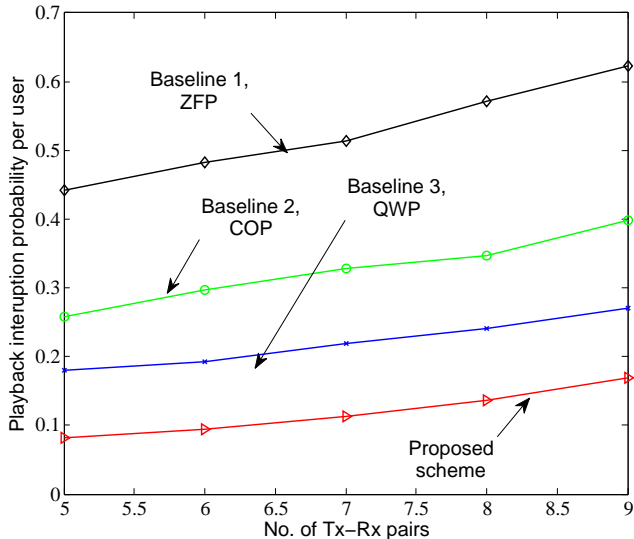In the simulations, we consider multimedia streaming in a K-pair MIMO interference network under the 802.11e WLAN

Fig. 9: Playback interruption probability per user versus no. of Tx-Rx pairs at average transmit SNR $= -5$ dB.
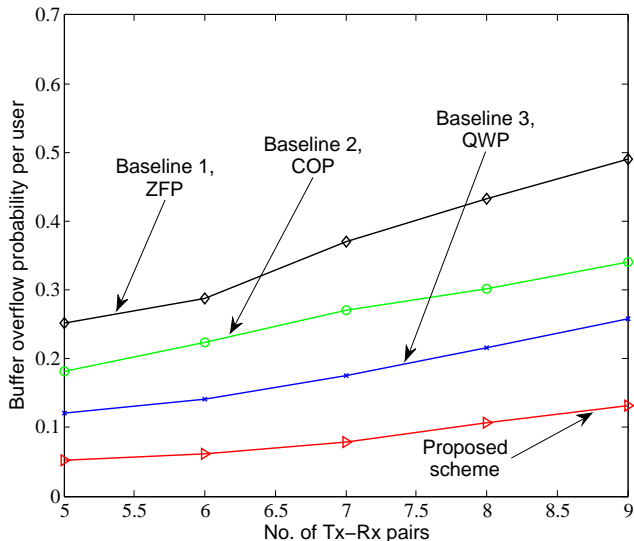

Fig. 10: Buffer overflow probability per user versus no. of Tx-Rx pairs at average transmit SNR $= -5$ dB.

setup as in [27]. The channel fading coefficient and the channel noise are complex Gaussian distributed. For the direct and the cross channel long-term path gain, we let $\frac{L_{kj}}{L_{kk}} = 0.1$ for all $k \neq j$ as in [28]. We consider constant bit rate video streaming for each mobile user with streaming rate equal to 1.5 Mbps as in [27]. The decision slot duration τ is 10 ms. The total bandwidth is 1MHz. Furthermore, we let $\gamma_k = \beta_k = \beta$ for all k and vary β to obtain different tradeoff curves. The mobile users adopt MMSE decorrelator as in (22) for all the baselines. We consider the average power cost (7), playback interruption probability (8) and buffer overflow probability (9) as the performance metrics for each multimedia streaming flow. The other system parameters are configured as: $\eta = 50$, $Q^l = 50$ Kbits and $Q^h = 150$ Kbits.

A. Playback Interruption and Buffer Overflow Probabilities versus Average Transmit SNR

Fig. 7 and Fig. 8 illustrates the playback interruption probability and buffer overflow probability per user versus average transmit SNR per pair. The proposed scheme achieves significant performance gain over all the baselines across a wide range of SNR values. It can also be observed that there exists a tradeoff between the playback interruption and buffer overflow probabilities, and we cannot decrease them both by adjusting the transmit power. From Fig. 7 and Fig. 8, we can see that the best SNR region for using our proposed algorithm is around -5 dB, where both the playback interruption and buffer overflow probabilities are relatively low, and there is also significant performance gain over the baselines.

B. Playback Interruption and Buffer Overflow Probabilities versus Number of Tx-Rx Pairs

Fig. 9 and Fig. 10 illustrates the playback interruption probability and buffer overflow probability per user versus the number of Tx-Rx pairs. The number of transmit antennas at the BS is K (which is equal to the number of Tx-Rx pairs) and the number of receive antennas at the mobile users is 2. It can be observed that our proposed scheme achieves significant performance gain over all the baselines across a wide range of the numbers of Tx-Rx pairs.

C. Performance Comparison of the Proposed Algorithm and the Optimal Solution

Fig. 11 illustrates the playback interruption and buffer overflow probabilities per user versus the carrier sensing distance δ for both the proposed Algorithm 1 and the brute-force value iteration (VIA) algorithm[12] [10]. It can be observed that the performance of our proposed algorithm is very close to that of the brute-force VIA algorithm and the performance gap becomes smaller as δ increases[13]. This is in accordance with the performance gap analysis in Theorem 4.

D. Computational Complexity Analysis

Table I illustrates the comparison of the MATLAB computational time of the proposed solution, the baselines and the brute-force value iteration algorithm [10]. Note that the computation time of all the algorithms increases as K increases, and this is a fair price to pay. The computational time of Baseline 1 is the smallest in all different K scenarios, but it has the worst performance. On the other hand, our proposed solution has a similar order of complexity growth w.r.t. K compared with Baseline 2/3 , but the proposed solution has much better performance.

---

[12]Note that the brute-force VIA [10] solves the discrete time Bellman equation in (11) and gives the optimal average cost.

[13]As δ increases, the worst-case cross channel path gain decreases according to the path loss model in Section II-C.
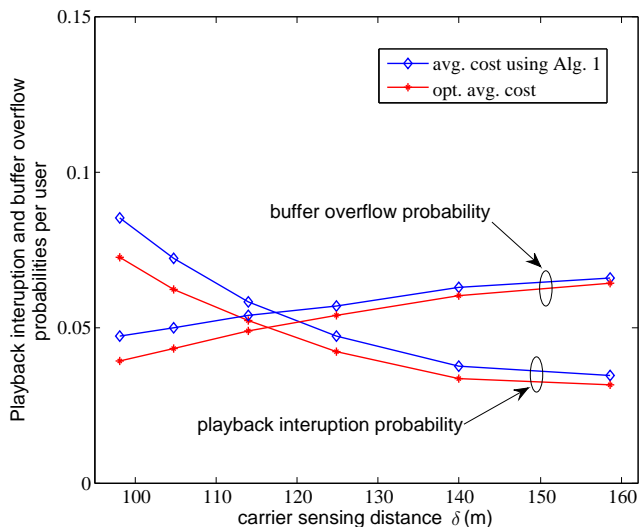
Fig. 11: Playback interruption and buffer overflow probabilities per user versus the carrier sensing distance at average transmit SNR $= -5$ dB, with $K = 4$, $N_t = 4$ and $N_r = 2$. The path loss model is given in Section II-C, where $G_r = G_t = 3$ dB and $\lambda = 0.125$ m (2.4 GHz carrier frequency). The direct channel path gain is -75 dBm.

	$K = 4$	$K = 6$	$K = 8$	$K = 10$
Baseline 1, ZFP	0.002s	0.003s	0.004s	0.006s
Baseline 2/3, COP/QWP	0.014s	0.023s	0.035s	0.051s
Proposed Scheme	0.052s	0.080s	0.125s	0.191s
Value Iteration Algorithm	657s	$> 10^4$s	$> 10^4$s	$> 10^4$s

TABLE I: Comparison of the MATLAB computational time of the proposed scheme, the baselines and the value iteration algorithm in one decision slot.

VII. SUMMARY

In this paper, we propose an asymptotically optimal dynamic precoder/decorrelator control to support multimedia streaming applications in MIMO interference networks. We formulate the associated stochastic optimization problem as an infinite horizon average cost MDP and derive the sufficient conditions for optimality. Using the weak interference property of the wireless network, we derive a closed-form approximate value function to the K-dimensional optimality equation and the associated error bound using perturbation analysis. Based on the closed-form approximate value function, we propose an asymptotically optimal low complexity precoder/decorrelator control algorithm and establish the performance gap between the optimal solution and the proposed low complexity solution. Numerical results show that the proposed scheme has much better performance than the other baselines.

APPENDIX A: PROOF OF THEOREM 1

Following *Proposition 4.6.1* of [10], the sufficient conditions for optimality of Problem 1 is that there exists a $(\theta^*, \{V^*(\mathbf{Q})\})$ that satisfies the following Bellman equation and V^* satisfies the transversality condition in (12) for all admissible control policy Ω and initial state $\mathbf{Q}(0)$:

$$\theta^* \tau + V^*(\boldsymbol{\chi}) \tag{30}$$
$$= \min_{\mathbf{F}, \mathbf{U}} \left[c(\mathbf{Q}, \mathbf{F}) \tau + \sum_{\boldsymbol{\chi}'} \Pr[\boldsymbol{\chi}'|\boldsymbol{\chi}, \mathbf{F}, \mathbf{U}] V^*(\boldsymbol{\chi}') \right]$$

$$= \min_{\mathbf{F}, \mathbf{U}} \left[c(\mathbf{Q}, \mathbf{F}) \tau + \sum_{\mathbf{Q}'} \sum_{\mathbf{H}'} \Pr[\mathbf{Q}'|\boldsymbol{\chi}, \mathbf{F}, \mathbf{U}] \Pr[\mathbf{H}'] V^*(\boldsymbol{\chi}') \right]$$

Taking expectation w.r.t. $\mathbf{H}$ on both sizes of the above equation and denoting $V^*(\mathbf{Q}) = \mathbb{E}[V^*(\boldsymbol{\chi})|\mathbf{Q}]$, we obtain the equivalent Bellman equation in (11) in Theorem 1.

APPENDIX B: PROOF OF COROLLARY 1

Let $\mathbf{Q}' = (Q_1', \cdots, Q_k') = \mathbf{Q}(t+1)$ and $\mathbf{Q} = (Q_1, \cdots, Q_k) = \mathbf{Q}(t)$. For the queue dynamics in (4) and sufficiently small τ, we have $Q_k' = Q_k - \mu_k \tau + R_k(\mathbf{H}, \mathbf{F}, \mathbf{U}_k)\tau, \forall k$. Therefore, if $V(\mathbf{Q})$ is of class $\mathcal{C}^2(\mathbb{R}_+^K)$, we have the following Taylor expansion on $V(\mathbf{Q}')$ in (11): $\mathbb{E}[V(\mathbf{Q}')|\mathbf{Q}] = V(\mathbf{Q}) + \sum_{k=1}^{K} \frac{\partial V(\mathbf{Q})}{\partial Q_k} [\mathbb{E}[R_k(\mathbf{H}, \mathbf{F}, \mathbf{U}_k)|\mathbf{Q}] - \mu_k]\tau + o(\tau)$. For notation convenience, let $T_{\boldsymbol{\chi}}(\theta, V, \mathbf{F}, \mathbf{U})$ and $T_{\boldsymbol{\chi}}^\dagger(\theta, V, \mathbf{F}, \mathbf{U})$ denote the *Bellman operators*:

$$T_{\boldsymbol{\chi}}(\theta, V, \mathbf{F}, \mathbf{U}) = T_{\boldsymbol{\chi}}^\dagger(\theta, V, \mathbf{F}, \mathbf{U}) + \nu G_{\boldsymbol{\chi}}(V, \mathbf{F}, \mathbf{U}) \tag{31}$$

for some smooth function $G_{\boldsymbol{\chi}}$ and $\nu = o(1)$ (which asymptotically goes to zero as τ goes to zero), and denote

$$T_{\boldsymbol{\chi}}^\dagger(\theta, V, \mathbf{F}, \mathbf{U}) = -\theta + c(\mathbf{Q}, \mathbf{F})$$
$$+ \sum_{k=1}^{K} \frac{\partial V(\mathbf{Q})}{\partial Q_k} [R_k(\mathbf{H}, \mathbf{F}, \mathbf{U}) - \mu_k] \tag{32}$$
$$T_{\boldsymbol{\chi}}(\theta, V) = \min_{\mathbf{F}, \mathbf{U}} T_{\boldsymbol{\chi}}(\theta, V, \mathbf{F}, \mathbf{U}),$$
$$T_{\boldsymbol{\chi}}^\dagger(\theta, V) = \min_{\mathbf{F}, \mathbf{U}} T_{\boldsymbol{\chi}}^\dagger(\theta, V, \mathbf{F}, \mathbf{U}) \tag{33}$$

Suppose (θ^*, V^*) satisfies the Bellman equation in (11) and (θ, V) satisfies the approximate Bellman equation in (14), we have for any $\mathbf{Q} \in \mathcal{Q}$,

$$\mathbb{E}[T_{\boldsymbol{\chi}}(\theta^*, V^*)|\mathbf{Q}] = 0, \quad \mathbb{E}\left[T_{\boldsymbol{\chi}}^\dagger(\theta, V)|\mathbf{Q}\right] = 0 \tag{34}$$

Then, we establish the following lemma.

Lemma 4: $\left|\mathbb{E}\left[T_{\boldsymbol{\chi}}(\theta, V)|\mathbf{Q}\right]\right| = o(1), \forall \boldsymbol{\chi}$, where $o(1)$ asymptotically goes to zero as τ goes to zero. ∎

Proof of Lemma 4: For any $\boldsymbol{\chi}$, we have $T_{\boldsymbol{\chi}}(\theta, V) = \min_{\mathbf{F}, \mathbf{U}} \left[T_{\boldsymbol{\chi}}^\dagger(\theta, V, \mathbf{F}, \mathbf{U}) + \nu G_{\boldsymbol{\chi}}(V, \mathbf{F}, \mathbf{U})\right] \geq \min_{\mathbf{F}, \mathbf{U}} T_{\boldsymbol{\chi}}^\dagger(\theta, V, \mathbf{F}, \mathbf{U}) + \nu \min_{\mathbf{F}, \mathbf{U}} G_{\boldsymbol{\chi}}(V, \mathbf{F}, \mathbf{U})$. On the other hand, $T_{\boldsymbol{\chi}}(\theta, V) \leq \min_{\mathbf{F}, \mathbf{U}} T_{\boldsymbol{\chi}}^\dagger(\theta, V, \mathbf{F}, \mathbf{U}) + \nu G_{\boldsymbol{\chi}}(V, \mathbf{F}^\dagger, \mathbf{U}^\dagger)$, where $(\mathbf{F}^\dagger, \mathbf{U}^\dagger) = \arg\min_{\mathbf{F}, \mathbf{U}} T_{\boldsymbol{\chi}}^\dagger(\theta, V, \mathbf{F}, \mathbf{U})$.

From (33) and (34), $\mathbb{E}\left[\min_{\mathbf{F}, \mathbf{U}} T_{\boldsymbol{\chi}}^\dagger(\theta, V, \mathbf{F}, \mathbf{U})|\mathbf{Q}\right] = \mathbb{E}\left[T_{\boldsymbol{\chi}}^\dagger(\theta, V)|\mathbf{Q}\right] = 0$. Since $T_{\boldsymbol{\chi}}^\dagger(\theta, V, \mathbf{F}, \mathbf{U})$ and $G_{\boldsymbol{\chi}}(V, \Omega^\dagger(\mathbf{Q}))$ are all smooth and bounded functions, we have $\left|\mathbb{E}\left[T_{\boldsymbol{\chi}}(\theta, V)|\mathbf{Q}\right]\right| = \mathcal{O}(\nu) = o(1)$ for any $\mathbf{Q} \in \mathcal{Q}$, where $o(1)$ asymptotically goes to zero as τ goes to zero. ∎

Finally, we prove the final result as follows.

Lemma 5: Suppose $\mathbb{E}[T_{\boldsymbol{\chi}}(\theta^*, V^*)|\mathbf{Q}] = 0$ for all $\mathbf{Q}$ together with the transversality condition in (12) has a unique solution (θ^*, V^*). If (θ, V) satisfies the approximate Bellman equation in (14) and the transversality condition in (12), then $|\theta - \theta^*| = o(1)$, $|V(\mathbf{Q}) - V^*(\mathbf{Q})| = o(1)$ for all $\mathbf{Q}$, where the error term $o(1)$ asymptotically goes to zero as τ goes to zero. ∎

Proof of Lemma 5: Suppose for some $\mathbf{Q}'$, we have $V(\mathbf{Q}') = V^*(\mathbf{Q}') + \alpha$ for some $\alpha \neq 0$. From Lemma 4, we have $|\mathbb{E}[T_{\boldsymbol{\chi}}(\theta, V)|\mathbf{Q}]| = o(1)$ for all $\mathbf{Q}$. Now let $\tau \to 0$, we have (θ, V) satisfies $\mathbb{E}[T_{\boldsymbol{\chi}}(\theta, V)|\mathbf{Q}] = 0$ for all $\mathbf{Q}$ and the transversality condition in (12). However, $V(\mathbf{Q}') \neq V^*(\mathbf{Q}')$ because of the assumption that $V(\mathbf{Q}') = V^*(\mathbf{Q}') + \alpha$. This

contradicts the condition that (θ^*, V^*) is a unique solution of $\mathbb{E}[T_\chi(\theta^*, V^*)|\mathbf{Q}] = 0$ for all $\mathbf{Q}$ and the transversality condition in (12). Hence, we must have $|V(\mathbf{Q}) - V^*(\mathbf{Q})| = o(1)$ for all $\mathbf{Q}$, where $o(1)$ asymptotically goes to zero as τ goes to zero. Similarly, we can establish $|\theta - \theta^*| = o(1)$. ∎

APPENDIX C: PROOF OF THEOREM 2

For simplicity of notation, we write $J(\mathbf{Q})$ in place of $J(\mathbf{Q}; L)$. We first establish the relationship between $J(\mathbf{Q})$ and $V(\mathbf{Q})$. We can observe that if $(c^\infty, \{J(\mathbf{Q})\})$ satisfies the PDE in (15), it also satisfies the approximate Bellman equation in (14). Furthermore, since $J(\mathbf{Q}) = \mathcal{O}(\sum_{k=1}^K Q_k)$, we have $\lim_{t\to\infty} \mathbb{E}^\Omega[J(\mathbf{Q}(t))] < \infty$ for any admissible policy Ω. Hence, $J(\mathbf{Q}) = \mathcal{O}(\sum_{k=1}^K Q_k)$ satisfies the transversality condition in (12).

Next, we show that the optimal control policy Ω^{J*} obtained by solving the PDE in (15) is an admissible control policy in the discrete time system as defined in Definition 2.

We first establish the following lemma:

Lemma 6: For any k, if $\frac{\partial J(\mathbf{Q}; L)}{\partial Q_k} > 0$ for sufficient large Q_k, then the optimal precoding matrix for user k obtained by solving (15) is $\mathbf{F}_k^{J*} = \mathbf{0}$. ∎

Proof of Lemma 6: For for sufficient large Q_k, let $\mathcal{I}_k = \{i : \frac{\partial J(\mathbf{Q};L)}{\partial Q_i} > 0\}$ ($k \in \mathcal{I}_k$), and let $\mathcal{I}_k^c = \{i : \frac{\partial J(\mathbf{Q};L)}{\partial Q_i} \leq 0\}$. Let $\mathbf{F}^{J*} = \{\mathbf{F}_i^{J*} : \forall i\}$ be the optimal precoding matrices obtained by solving the PDE in (15). Suppose some $\mathbf{F}_i^{J*} \neq \mathbf{0}$ ($i \in \mathcal{I}_k' \subset \mathcal{I}_k$). Denote $\widetilde{\mathbf{F}}^{J*} = \{\widetilde{\mathbf{F}}_i^{J*} = \mathbf{F}_i^{J*} : i \notin \mathcal{I}_k'\} \cup \{\widetilde{\mathbf{F}}_i^{J*} = \mathbf{0} : i \in \mathcal{I}_k'\}$. Denote the objective function in (15) for given χ as

$$f_\chi(\mathbf{F}) = \sum_{i=1}^K \left(\text{Tr}\left(\mathbf{F}_i \mathbf{F}_i^\dagger\right) + \frac{\partial J(\mathbf{Q}; L)}{\partial Q_i}(R_i(\mathbf{H}, \mathbf{F}))\right) \quad (35)$$

where the optimal MMSE receiver [17] is adopted at the receiver and $R_i(\mathbf{H}, \mathbf{F}) = W\log_2 \det(\mathbf{I} + L_{ii}\mathbf{H}_{ii}\mathbf{F}_i\mathbf{F}_i^\dagger\mathbf{H}_{ii}^\dagger(\sum_{j\neq i} L_{ij}\mathbf{H}_{ij}\mathbf{F}_j\mathbf{F}_j^\dagger\mathbf{H}_{ij}^\dagger + \mathbf{I})^{-1})$. Then, we have

$$f_\chi(\mathbf{F}^{J*}) \quad (36)$$
$$= \sum_{i\in\mathcal{I}_k} \left(\text{Tr}\left(\mathbf{F}_i^{J*}(\mathbf{F}_i^{J*})^\dagger\right) + \frac{\partial J(\mathbf{Q}; L)}{\partial Q_i}\left(R_i\left(\mathbf{H}, \mathbf{F}^{J*}\right)\right)\right)$$
$$+ \sum_{i\notin\mathcal{I}_k} \left(\text{Tr}\left(\mathbf{F}_i^{J*}(\mathbf{F}_i^{J*})^\dagger\right) + \frac{\partial J(\mathbf{Q}; L)}{\partial Q_i}\left(R_i\left(\mathbf{H}, \mathbf{F}^{J*}\right)\right)\right)$$
$$\overset{(a)}{\geq} \sum_{i\notin\mathcal{I}_k} \left(\text{Tr}\left(\mathbf{F}_i^{J*}(\mathbf{F}_i^{J*})^\dagger\right) + \frac{\partial J(\mathbf{Q}; L)}{\partial Q_i}\left(R_i\left(\mathbf{H}, \mathbf{F}^{J*}\right)\right)\right)$$
$$\overset{(b)}{>} \sum_{i\notin\mathcal{I}_k} \left(\text{Tr}\left(\widetilde{\mathbf{F}}_i^{J*}(\widetilde{\mathbf{F}}_i^{J*})^\dagger\right) + \frac{\partial J(\mathbf{Q}; L)}{\partial Q_i}\left(R_i\left(\mathbf{H}, \widetilde{\mathbf{F}}^{J*}\right)\right)\right)$$
$$= f_\chi(\widetilde{\mathbf{F}}^{J*})$$

where (a) is due to $\text{Tr}(\mathbf{F}_i^{J*}(\mathbf{F}_i^{J*})^\dagger) + \frac{\partial J(\mathbf{Q};L)}{\partial Q_i}(R_i(\mathbf{H}, \mathbf{F}^{J*})) \geq 0$ for $i \in \mathcal{I}_k$, (b) is due to $\text{Tr}(\mathbf{F}_i^{J*}(\mathbf{F}_i^{J*})^\dagger) = \text{Tr}(\widetilde{\mathbf{F}}_i^{J*}(\widetilde{\mathbf{F}}_i^{J*})^\dagger)$ and $R_i(\mathbf{H}, \mathbf{F}^{J*}) \leq R_i(\mathbf{H}, \widetilde{\mathbf{F}}^{J*})$ for $i \notin \mathcal{I}_k$. Therefore, from (36), $\widetilde{\mathbf{F}}^{J*}$ achieves smaller objective than $\mathbf{F}^{J*}$, which contradicts that $\mathbf{F}^{J*}$ is the optimal solution. Therefore, for $i \in \mathcal{I}_k$ ($k \in \mathcal{I}_k$), the optimal precoding matrix is $\mathbf{0}$. ∎

Define the *semi-invariant moment generating function* of $R_k(\mathbf{H}, \Omega^{J*}(\chi)) - \mu_k$ as $\phi_k(r, \mathbf{Q}) = $

$\ln\left(\mathbb{E}\left[e^{(R_k(\mathbf{H}, \Omega^{J*}(\chi)) - \mu_k)r}|\mathbf{Q}\right]\right)$. According to Lemma 6, we have $\mathbb{E}[R_k(\mathbf{H}, \Omega^{J*}(\chi)) - \mu_k|\mathbf{Q}] = -\mu_k < 0$ when $Q_k > \overline{Q}_k$ for some large $\overline{Q}_k$. Hence, $\phi_k(r, \mathbf{Q})$ will have a unique positive root $r_k^*(\mathbf{Q})$ ($\phi_k(r_k^*(\mathbf{Q}), \mathbf{Q}) = 0$) [14]. Let $r_k^* = r_k^*(\overline{\mathbf{Q}})$, where $\overline{\mathbf{Q}} = (\overline{Q}_1, \ldots, \overline{Q}_K)$. We then have the following lemma on the tail distribution Q_k, $\Pr[Q_k \geq x]$.

Lemma 7 (Kingman Bound [14]): $P_k(x) \triangleq \Pr[Q_k \geq x] \leq e^{-r_k^* x}$, if $x \geq \overline{x}_k$ for sufficiently large $\overline{x}_k$. ∎

Finally, we check whether Ω^{J*} stabilizes the system according to the definition of the admissible control policy in Definition 2 as follows: $\mathbb{E}^{\Omega^{J*}}[J(\mathbf{Q})] \leq C\sum_{k=1}^K \mathbb{E}^{\Omega^{J*}}[Q_k] = C\sum_{k=1}^K\left[\int_0^\infty \Pr[Q_k > s]\,\text{d}s\right] \leq C\sum_{k=1}^K\left[\overline{x}_k + \int_{\overline{x}_k}^\infty e^{-r_k^* s}\text{d}s\right] < \infty$ for some positive constant C. Therefore, Ω^{J*} is an admissible control policy and we have $V(\mathbf{Q}) = J(\mathbf{Q})$ and $\theta = c^\infty$. Furthermore, using Corollary 1, we have $V^*(\mathbf{Q}) = J(\mathbf{Q}) + o(1)$ and $\theta^* = c^\infty + o(1)$ for sufficiently small τ.

APPENDIX D: PROOF OF LEMMA 1

1) Proof of the decomposable structure of the base PDE: In the base PDE, since $L_{kj} = 0$ for all $k, j, k \neq j$, the associated PDE becomes:

$$\mathbb{E}\Big[\min_{\mathbf{F}, \mathbf{U}} \Big[\sum_{k=1}^K \left(\text{Tr}\left(\mathbf{F}_k\mathbf{F}_k^\dagger\right) + \gamma_k e^{-\eta[Q_k - Q^l]^+} + \beta_k e^{-\eta[Q^h - Q_k]^+}\right)$$
$$+ \frac{\partial J(\mathbf{Q}; 0)}{\partial Q_k}\left(R_k^0(\mathbf{H}, \mathbf{F}_k, \mathbf{U}_k) - \mu_k\right)\Big]\Big|\mathbf{Q}\Big] - c^\infty = 0 \quad (37)$$

with boundary condition $J_k(Q_k^*) = 0$, for some Q_k^*, where we denote $R_k^0(\mathbf{H}, \mathbf{F}_k, \mathbf{U}_k) = W\log_2 \det(\mathbf{I} + L_{kk}\mathbf{U}_k^\dagger\mathbf{H}_{kk}\mathbf{F}_k\mathbf{F}_k^\dagger\mathbf{H}_{kk}^\dagger\mathbf{U}_k)$. We have the following lemma establishing the decomposable structure of the $J(\mathbf{Q}; 0)$ and c^∞ in (37).

Lemma 8 (Decomposed Optimality Equation): Suppose there exist c_k^∞ and $J_k(Q_k) \in \mathcal{C}^2(\mathbb{R}_+)$ that solve the following per-flow PDE:

$$\mathbb{E}\Big[\min_{\mathbf{F}_k} \left[\text{Tr}(\mathbf{F}_k\mathbf{F}_k^\dagger) + \gamma_k e^{-\eta[Q_k - Q^l]^+} + \beta_k e^{-\eta[Q^h - Q_k]^+}\right.$$
$$+ J_k'(Q_k)\left(R_k^0(\mathbf{H}, \mathbf{F}_k, \mathbf{U}_k) - \mu_k\right)\Big]\Big|\mathbf{Q}\Big] - c_k^\infty = 0 \quad (38)$$

Then, $J(\mathbf{Q}; 0) = \sum_{k=1}^K J_k(Q_k)$ and $c^\infty = \sum_{k=1}^K c_k^\infty$ satisfy (37). ∎

Lemma 8 can be proved using the fact that the dynamics of the playback buffer are decoupled when $L = 0$. The details are omitted for conciseness.

2) Solving the per-flow PDE: We first write $\mathbf{F}_k = \widetilde{\mathbf{F}}_k \mathbf{\Sigma}_k$, where $\widetilde{\mathbf{F}}_k = [\mathbf{f}_{k1}, \ldots, \mathbf{f}_{kd}] \in \mathbb{C}^{N_t \times d}$ with $\|\mathbf{f}_{ki}\| = 1$ ($\forall i = 1, \ldots, d$), and $\mathbf{\Sigma}_k = \text{diag}(p_{k1}, \ldots, p_{kd})$ where p_{ki} is the power allocated for the i-th data stream. Let the singular value decomposition of the channel matrix be $\mathbf{H}_{kk} = \mathbf{M}_k\mathbf{\Lambda}_k\mathbf{N}_k^\dagger$, where $\mathbf{M}_k \in \mathbb{C}^{N_r \times N_r}$ and $\mathbf{N}_k \in \mathbb{C}^{N_t \times N_t}$ are unitary matrices and $\mathbf{\Lambda}_k \in \mathbb{R}^{N_r \times N_t}$ whose diagonal elements $\sigma_{k1} \geq \cdots \geq \sigma_{kd}$ are the singular values of $\mathbf{H}_{kk}$ and the off-diagonal elements are zero. Therefore, the problem in the base PDE (38) becomes:

$$\min_{\substack{p_{k1}, \ldots, p_{kd}, \\ \widetilde{\mathbf{F}}_k, \mathbf{U}_k}} \sum_{i=1}^d p_{ki} + J_k'(Q_k)W\log_2 \det\Big(\mathbf{I}$$
$$+ L_{kk}\mathbf{U}_k^\dagger\mathbf{M}_k\mathbf{\Lambda}_k\mathbf{N}_k^\dagger\widetilde{\mathbf{F}}_k\mathbf{\Sigma}_k\mathbf{\Sigma}_k^\dagger\widetilde{\mathbf{F}}_k^\dagger\mathbf{N}_k\mathbf{\Lambda}_k^\dagger\mathbf{M}_k^\dagger\mathbf{U}_k\Big) \quad (39)$$

The above problem is the classical MIMO beamforming control problem [29] and the optimal $\widetilde{\mathbf{F}}_k^*$ is the first d columns

of $\mathbf{N}_k$, the optimal $\widetilde{\mathbf{U}}_k^*$ is the first d columns of $\mathbf{M}_k$, and the optimal power allocation is given by

$$p_{ki}^*(\sigma_{ki}) = \left(-\frac{J_k'(Q_k)W}{\ln 2} - \frac{1}{L_{kk}\sigma_{ki}^2} \right)^+ \tag{40}$$

We next calculate the expectations involved in (38). Specifically, substituting the optimal precoding matrix $\widetilde{\mathbf{F}}_k^*$, $\mathbf{U}_k^*$ and power p_{ki}^* into (38), we obtain that

$$\mathbb{E}\left[\mathrm{Tr}\left(\mathbf{F}_k^*(\mathbf{F}_k^*)^\dagger \right) \right] = \mathbb{E}\left[\sum_{i=1}^{d} p_{ki}^*(\sigma_{ki}) \right] = d\mathbb{E}\left[p_{k1}^*(\sigma_{k1}) \right] \tag{41}$$

$$\mathbb{E}\left[R_k^0\left(\mathbf{H}, \mathbf{F}_k^*, \mathbf{U}_k^* \right) \right] = \mathbb{E}\left[W \sum_{i=1}^{d} \log_2\left(1 + L_{kk}\sigma_{ki}^2 p_{ki}^*(\sigma_{ki}) \right) \right]$$
$$= d\mathbb{E}\left[W \log_2\left(1 + L_{kk}\sigma_{k1}^2 p_{k1}^*(\sigma_{k1}) \right) \right] \tag{42}$$

which depend on the distribution of one of the unordered singular values. Let $b = \max\{N_t, N_r\}$. According to [30], the distribution of any σ_{ki}^2 is given by: $f_{\sigma_{ki}^2}(x) = \frac{x^{d-b}e^x}{d} \sum_{n=1}^{d} \varphi_n^2(x)$, where $\varphi_{n+1}(x)$ is given by $\varphi_{n+1}(x) = \left[\frac{1}{n!(n+b-d)!} \right]^{1/2} \frac{\mathrm{d}^n}{\mathrm{d}x^n}(e^{-x}x^{n+b-d}) = \left[\frac{1}{n!(n+b-d)!} \right]^{1/2} \sum_{l=0}^{n} A_{n,l}(-1)^l C_n^l e^{-x}x^{b-d+l}$, with $A_{n,l} = 1$ if $l = n$ and $A_{n,l} = \prod_{r=0}^{n-l-1}(n-r+b-d)$ if $l < n$, and C_n^l is the Binomial coefficient. Therefore, the distribution of any σ_{ki}^2 can be rewritten as $f_{\sigma_{ki}^2}(x) = \frac{x^{b-d}e^{-x}}{d} \sum_{n=0}^{d-1} \frac{1}{n!(n+b-d)!} \left[\sum_{l=0}^{n} A_{n,l}(-1)^l C_n^l x^l \right]^2 = \frac{x^{b-d}e^{-x}}{d} \sum_{n=0}^{d-1} b_n \left[\sum_{l=0}^{n} a_{n,l,l}x^{2l} + \sum_{l=0}^{n}\sum_{j>l} 2a_{n,l,j}x^{l+j} \right]$, where we denote $b_n = \frac{1}{n!(n+b-d)!}$, and $a_{n,l,j} = (A_{n,l}C_n^l)^2$ when $l = j$ and $a_{n,l,j} = A_{n,l}A_{n,j}(-1)^{l+j}C_n^l C_n^j$ when $j > l$. We further denote $s \triangleq b - d$ and $t_k \triangleq \frac{-\ln 2}{WL_{kk}}$. We then calculate (41) and (42) as follows:

$$d\mathbb{E}\left[p_{k1}^*(\sigma_{k1}) \right] = \frac{1}{L_{kk}} \sum_{n=0}^{d-1} b_n \left[\sum_{l=0}^{n} a_{n,l,l} \left[\frac{J_k'(Q_k)}{t_k} \right. \right. \tag{43}$$
$$G\left(1+2l+s, \frac{t_k}{J_k'(Q_k)} \right) - G\left(2l+s, \frac{t_k}{J_k'(Q_k)} \right) \right] + \sum_{l=0}^{n}\sum_{j>l} 2a_{n,l,j} \left[\frac{J_k'(Q_k)}{t_k} G\left(1+l+j+s, \frac{t_k}{J_k'(Q_k)} \right) - G\left(l+j+s, \frac{t_k}{J_k'(Q_k)} \right) \right] \right]$$

$$d\mathbb{E}\left[W \log_2\left(1 + L_{kk}\sigma_{k1}^2 p_{k1}^*(\sigma_{k1}) \right) \right] = \frac{W}{\ln 2} \sum_{n=0}^{d-1} b_n \left[\sum_{l=0}^{n} a_{n,l,l} \right.$$
$$M\left(\{1,1\}, \{0,0,1+2l+s\}, \frac{t_k}{J_k'(Q_k)} \right) \tag{44}$$
$$+ \sum_{l=0}^{n}\sum_{j>l} 2a_{n,l,j} M\left(\{1,1\}, \{0,0,1+l+j+s\}, \frac{t_k}{J_k'(Q_k)} \right) \right]$$

where[14] $G(m,x) = G_a(m,x)$ (Gamma function) if $x > 0$ and equals to zero otherwise. $M(\{\},\{\},x) = M_g(\{\},\{\},x)$ if $x > 0$ and equals to zero otherwise. We then calculate c_k^∞. Assuming $e^{\eta(Q^l-Q^h)} < \frac{\gamma_k}{\beta_k} < e^{\eta(Q^h-Q^l)}$, and we define the following *target* operating queue regime $Q_k^\star$ (achieving the minimum of the per-stage cost function $c_k(Q_k, \mathbf{F}_k)$ within

[14] $M_g(\{a_1, \ldots, a_n\}, \{b1, \ldots, b_m\}, z) = \frac{1}{2\pi i} \int_{\mathcal{L}} \frac{\prod_{k=1}^{m} \Gamma(b_k-s)}{\prod_{k=1}^{n} \Gamma(a_k-s)} z^s \mathrm{d}s$ is the Meijer G-function, where $\Gamma(a) = G_a(a,0)$. $G_a(a,x) = \int_x^\infty t^{a-1}e^{-t}\mathrm{d}t$ is the incomplete gamma function.

the domain (Q^l, Q^h) for given precoding matrix $\mathbf{F}_k$:

$$Q_k^\star = \min_{Q_k} c_k(Q_k, \mathbf{F}_k) = \frac{Q^l + Q^h}{2} + \frac{1}{2\eta} \ln\frac{\gamma_k}{\beta_k} \in (Q^l, Q^h) \tag{45}$$

To satisfy boundary condition $J_k(Q_k^\star) = 0$, we require that $c_k^\infty = \mathrm{R.H.S.of}\ (43)\big|_{Q_k=Q_k^\star} + \gamma_k e^{-\eta[Q_k^\star-Q^l]^+} + \beta_k e^{-\eta[Q^h-Q_k^\star]^+}$ and $\mathbb{E}\left[R_k^0\left(\mathbf{H}, \mathbf{F}_k^*, \mathbf{U}_k^* \right) \right]\big|_{Q_k=Q_k^\star} = \mathrm{R.H.S.of}\ (44)\big|_{Q_k=Q_k^\star} = \mu_k$. Therefore, we have

$$c_k^\infty = \frac{1}{L_{kk}} \sum_{n=0}^{d-1} b_n \left[\sum_{l=0}^{n} a_{n,l,l} \left[\frac{\lambda_k}{t_k} G\left(1+2l+s, \frac{t_k}{\lambda_k} \right) - G\left(2l+s, \frac{t_k}{\lambda_k} \right) \right] \right.$$
$$+ \sum_{l=0}^{n}\sum_{j>l} 2a_{n,l,j} \left[\frac{\lambda_k}{t_k} G\left(1+l+j+s, \frac{t_k}{\lambda_k} \right) - G\left(l+j+s, \frac{t_k}{\lambda_k} \right) \right] \right]$$
$$+ \gamma_k e^{-\eta[Q_k^\star-Q^l]} + \beta_k e^{-\eta[Q^h-Q_k^\star]} \tag{46}$$

where $\lambda_k \in \mathbb{R}_-$ satisfies $\frac{W}{\ln 2} \sum_{n=0}^{d-1} b_n [\sum_{l=0}^{n} a_{n,l,l} M(\{1,1\}, \{0,0,1+2l+s\}, \frac{t_k}{\lambda_k}) + \sum_{l=0}^{n}\sum_{j>l} 2a_{n,l,j} M(\{1,1\}, \{0,0,1+l+j+s\}, \frac{t_k}{\lambda_k})] = \mu_k$. Substituting the results on the expectations in (43) and (44), and the result on c_k^∞ in (46) into (38), we can obtain the following fixed point equation determining $J_k'(Q_k)$:

$$g(Q_k, J_k') = 0 \tag{47}$$

where we denote $g(Q_k, J_k') \triangleq \frac{1}{L_{kk}} \sum_{n=0}^{d-1} b_n \left[\sum_{l=0}^{n} a_{n,l,l} \left[\frac{J_k'}{t_k} G(1+2l+s, \frac{t_k}{J_k'}) - G(2l+s, \frac{t_k}{J_k'}) \right] + \sum_{l=0}^{n}\sum_{j>l} 2a_{n,l,j} \left[\frac{J_k'}{t_k} G(1+l+j+s, \frac{t_k}{J_k'}) - G(l+j+s, \frac{t_k}{J_k'}) \right] \right] + \gamma_k e^{-\eta[Q_k-Q^l]^+} + \beta_k e^{-\eta[Q^h-Q_k]^+} + J_k'(\frac{W}{\ln 2} \sum_{n=0}^{d-1} [\sum_{l=0}^{n} a_{n,l,l} M(\{1,1\}, \{0,0,1+2l+s\}, \frac{t_k}{J_k'}) + \sum_{l=0}^{n}\sum_{j>l} 2a_{n,l,j} M(\{1,1\}, \{0,0,1+l+j+s\}, \frac{t_k}{J_k'})] - \mu_k) - c_k^\infty$. It can be shown that for fixed $Q_k \in [0, Q_k^*]$, $g(Q_k, J_k')$ is strictly increasing w.r.t. J_k' over $(-\infty, \lambda_k]$ and $g(Q_k, \lambda_k) \geq 0$. Then, it follows that $g(Q_k, J_k') = 0$ has a unique solution over $J_k' \in (-\infty, \lambda_k]$. Similarly, it can be shown that for fixed $Q_k \in [Q_k^*, \infty)$, $g(Q_k, J_k')$ is strictly decreasing w.r.t. J_k' over $[\lambda_k, \infty)$ and $g(Q_k, \lambda_k) \geq 0$. Then, it follows that $g(Q_k, J_k') = 0$ has a unique solution over $J_k' \in [\lambda_k, \infty)$.

3) Asymptotic property of $J_k(Q_k)$: based on the above analysis on the behavior of $g(Q_k, J_k')$, we have that for sufficiently large Q_k, $J_k'(Q_k)$ become positive and the fixed point equation is simplified as follows: $\beta_k - J_k'(\infty)\mu_k - c_k^\infty = 0$. Assuming $\beta_k > c_k^\infty$, then $J_k'(\infty) = \frac{\beta_k-c_k^\infty}{\mu_k} > 0$. Denote $C_k = \frac{\beta_k-c_k^\infty}{\mu_k}$. Thus, we have that $J_k(Q_k) = C_k Q_k$, as $Q_k \to \infty$.

APPENDIX E: PROOF OF THEOREM 3

Taking the first order Taylor expansion of the L.H.S. of the PDE in (15) at $L_{kj} = 0$ ($\forall k, j$), $\mathbf{F}_k = \mathbf{F}_k^*$ and $\mathbf{U}_k = \mathbf{U}_k^*$ (where $\mathbf{F}_k^*$ and $\mathbf{U}_k^*$ are the optimal control actions solving the per-flow PDE in (38)), and using parametric optimization analysis [31], we have the following result regarding the approximation error:

$$J(\mathbf{Q}; L) - J(\mathbf{Q}; 0) = \sum_{k=1}^{K}\sum_{j \neq k} L_{kj}\widetilde{J}_{kj}(\mathbf{Q}) + \mathcal{O}(L^2) \tag{48}$$

where $\widetilde{J}_{kj}(\mathbf{Q})$ is meant to capture the coupling terms in $J(\mathbf{Q}; L)$ which satisfies the following PDE:

$$\sum_{i=1}^{K} \left(\mathbb{E}\left[R_i^0\left(\mathbf{H}_{ii}, \mathbf{F}_i^*, \mathbf{U}_i^*\right) | Q_i \right] - \mu_i \right) \frac{\partial \widetilde{J}_{kj}(\mathbf{Q})}{\partial Q_i}$$

$$+ \mathbb{E}\left[J_k'(Q_k) \frac{\partial R_k\left(\mathbf{H}, \mathbf{F}^*, \mathbf{U}_k^*\right)}{\partial L_{kj}} \Bigg|_{L=0} \Bigg| \mathbf{Q} \right] = 0 \qquad (49)$$

with boundary condition $\widetilde{J}_{kj}(\mathbf{Q})\big|_{Q_i=Q_i^\star} = 0$ or $\widetilde{J}_{kj}(\mathbf{Q})\big|_{Q_j=Q_j^\star} = 0$. We next calculate the two expectations involved in the above equation. According to the analysis of the fixed point equation in (47) in Appendix D.2, $J_k'(Q_k)$ decreases and approaches to $-\infty$ as Q_k decreases on the domain $(-\infty, Q_k^\star]$, while $J_k'(Q_k)$ increases and approaches to ∞ as Q_k increases on the domain $[Q_k^\star, \infty)$. Therefore, we calculate the expectations in (49) by taking into account of the queue regions. For the first expectation, according to (18) and (42), we have that if $Q_i \geq Q_i^\star$, as Q_i goes to infinity, then

$$\mathbb{E}\left[R_i^0\left(\mathbf{H}_{ii}, \mathbf{F}_i^*, \mathbf{U}_i^*\right) | Q_i \right] = 0, \quad \text{for large } Q_i \qquad (50)$$

since the water level in (40) which is determined by $-J_k'(Q_k)$ becomes negative (as $Q_i \to \infty$). If $Q_i < Q_i^\star$, $J_k'(Q_k)$ approaches $-\infty$ as Q_i decreases. Based on the asymptotic behavior of the Gamma function and the Meijer-G function: $G(n, \frac{a}{y}) = (n-1)! + o(1)$, $M(\{1,1\}, \{0,0,N\}, \frac{1}{ay}) = (N-1)! \ln ay + (N-1)! P_g^0(N) + o(1)$ for a, y with the same sign, where $P_g^0(x)$ is the Polygamma function. From (47), we have

$$-c_k^1 J_k'(Q_k) - c_k^2 + \beta_k + J_k'(Q_k)\left[c_k^1 \ln(-J_k'(Q_k)) + c_k^3 - \mu_k \right]$$
$$= c_k^\infty \qquad (51)$$

where we denote c_k^1, c_k^2, c_k^3 as follows[15]:

$$c_k^1 \triangleq \qquad\qquad\qquad\qquad\qquad\qquad\qquad\qquad (52)$$
$$\frac{1}{L_{kk}} \sum_{n=0}^{d-1} b_n \left[\sum_{l=0}^{n} a_{n,l,l} \frac{(2l+s)!}{-t_k} + \sum_{l=0}^{n}\sum_{j>l} 2a_{n,l,j} \left[\frac{(l+j+s)!}{-t_k} \right] \right]$$

$$c_k^2 \triangleq \qquad\qquad\qquad\qquad\qquad\qquad\qquad\qquad (53)$$
$$\frac{1}{L_{kk}} \sum_{n=0}^{d-1} b_n \left[\sum_{l=0}^{n} a_{n,l,l}(2l+s-1)! + \sum_{l=0}^{n}\sum_{j>l} 2a_{n,l,j}(l+j+s-1)! \right]$$

$$c_k^3 \triangleq \frac{W}{\ln 2} \sum_{n=0}^{d-1} b_n \left(\sum_{l=0}^{n} a_{n,l,l}(2l+s)! \left[-\ln(-t_k) + P_g^0(1+2l+s) \right] \right.$$
$$\left. + \sum_{l=0}^{n}\sum_{j>l} 2a_{n,l,j}(l+j+s)! \left[-\ln(-t_k) + P_g^0(1+l+j+s) \right] \right) \qquad (54)$$

where c_k^1 and c_k^2 are positive. Therefore, for sufficiently small Q_k, we can rewrite (51) as

$$-c_k^1 D_k - c_k^2 + \beta_k + D_k \left[c_k^1 \ln(-D_k) + c_k^3 - \mu_k \right] = c_k^\infty \quad (55)$$

where we use D_k to represent $J_k'(Q_k)$ for large Q_k. Note that (55) has a unique solution if $\beta_k > c_k^\infty$. Therefore, for the first expectation in (49), for small Q_i, we have

$$\mathbb{E}\left[R_i^0\left(\mathbf{H}_{ii}, \mathbf{F}_i^*, \mathbf{U}_i^*\right) | Q_i \right] = c_i^1 \ln(-D_i) + c_i^3, \quad \text{for small } Q_i \qquad (56)$$

Furthermore, $c_i^1 \ln(-D_i) + c_i^3 - \mu_i > 0$ according to (55). For the second expectation in

[15] $P_g^0(x) = (\log(\Gamma(x)))'$ is the polygamma function.

(49), we have $\frac{\partial R_k\left(\mathbf{H}, \mathbf{F}^*, \mathbf{U}_k^*\right)}{\partial L_{kj}}\Big|_{L=0} = -\text{Tr}((\mathbf{I} + L_{kk}(\mathbf{U}_k^*)^\dagger \mathbf{H}_{kk}\mathbf{F}_k^*(\mathbf{F}_k^*)^\dagger \mathbf{H}_{kk}^\dagger \mathbf{U}_k^*)^{-1} L_{kk}(\mathbf{U}_k^*)^\dagger \mathbf{H}_{kk}\mathbf{F}_k^*(\mathbf{F}_k^*)^\dagger \mathbf{H}_{kk}^\dagger \mathbf{H}_{kj} \mathbf{F}_j^*(\mathbf{F}_j^*)^\dagger \mathbf{H}_{kj}^\dagger \mathbf{U}_k^*)$. Substituting $\mathbf{F}_k^*$ and $\mathbf{U}_k^*$ in (38), we obtain

$$\mathbb{E}\left[\frac{\partial R_k\left(\mathbf{H}, \mathbf{F}^*, \mathbf{U}_k^*\right)}{\partial L_{kj}}\Bigg|_{L=0} \Bigg| \mathbf{Q} \right]$$
$$= -\mathbb{E}\left[\sum_{n=1}^{d} \frac{L_{kk} p_{kn}^*(\sigma_n)\sigma_n^2}{L_{kk} p_{kn}^*(\sigma_n)\sigma_n^2 + 1} p_{jn}^*(\sigma_n) \Bigg| \mathbf{Q} \right] \qquad (57)$$

Similarly, if either Q_k or Q_j is sufficiently large, (57) equals to zero. Otherwise, (57) equals to $\frac{-1}{d}\left(c_k^1 D_k + c_k^2 \right) \cdot \frac{\ln 2}{D_k W}\left(c_j^1 D_j + c_j^2 \right) \triangleq G_{kj}$. Denote $G_k \triangleq c_k^1 \ln(-D_k) + c_k^3 - \mu_k$. Combining (50) and (56), according to Section *3.8.1.2* of [32] and taking into account of the boundary conditions, by solving (49) we have $\widetilde{J}_{kj}(\mathbf{Q}) = o(1)$ if either $Q_k \geq Q_k^\star$ or $Q_j \geq Q_j^\star$, and $\widetilde{J}_{kj}(\mathbf{Q}) = -\frac{D_k G_{kj}}{2 G_k}(Q_k - Q_k^\star) - \frac{D_k G_{kj}}{2 G_j}(Q_j - Q_j^\star) + o(Q_k) + o(Q_j)$ otherwise. Substituting it into (48) and denoting $E_{kj} = \frac{D_k G_{kj}}{2 G_k}$, we obtain the approximation error in Theorem 3.

APPENDIX F: PROOF OF LEMMA 3

1) *Convergence property:* The proof follows similar approach as in [17] by showing (23) and (24) have the same KKT conditions at the stationary point $\{\mathbf{F}(\infty), \mathbf{Z}(\infty), \mathbf{K}(\infty)\}$. Details are omitted due to page limit.

2) *Asymptotically optimality:* we next prove the asymptotically property of Algorithm 1. Denote the objective function in (23) as $f(\mathbf{F}, L)$. We have the following lemma on the convexity for $f(\mathbf{F}, L)$.

Lemma 9 (Convexity of $f(\mathbf{F}, L)$ for Sufficiently Small L): $f(\mathbf{F}, L)$ is a convex function of $\mathbf{F} = \{\mathbf{F}_k : \forall k\}$ when L is sufficiently small. ∎

Proof: According to [33], we have the following argument regarding the convexity of a function $f(\mathbf{x})$: given any two different feasible points $\mathbf{x}_1$ and $\mathbf{x}_2$, define $g(t) = f(t\mathbf{x}_1 + (1-t)\mathbf{x}_2)$, $0 \leq t \leq 1$, then $f(\mathbf{x})$ is a convex function of $\mathbf{x}$ if and only if $g(t)$ is a convex function of t, which is equivalent to $\frac{d^2 g(t)}{dt^2} \geq 0$ for $0 \leq t \leq 1$.

Therefore, we consider the convex combination of two different feasible solutions $\mathbf{F}^{(1)} = \{\mathbf{F}_k^{(1)} : \forall k\}$ and $\mathbf{F}^{(2)} = \{\mathbf{F}_k^{(2)} : \forall k\}$ as follows: $\mathbf{F}^c = \{\mathbf{F}_k^c = t\mathbf{F}_k^{(1)} + (1-t)\mathbf{F}_k^{(2)} : \forall k\}$ and $0 \leq t \leq 1$. Denote $\mathbf{F}_{-k} = \{\mathbf{F}_j : \forall j \neq k\}$, $\mathbf{G}_k(\mathbf{F}_{-k}) = \mathbf{I} + \sum_{j\neq k} L_{kj}\mathbf{H}_{kj}\mathbf{F}_j\mathbf{F}_j^\dagger \mathbf{H}_{kj}^\dagger$, $\mathbf{Y}_k = \mathbf{F}_k^{(1)} - \mathbf{F}_k^{(2)}$ and $a_k = \frac{W}{\ln 2} \frac{\partial \widetilde{V}(\mathbf{Q})}{\partial Q_k}$. W.l.o.g, we assume $a_k \leq 0$ for all k (since for $a_k > 0$, the associated optimal $\mathbf{F}_k = \mathbf{0}$, and thus we can focus on those Tx-Rx pair j such that $a_j \leq 0$. See Lemma 6 in Appendix C for the detailed proof), then the second order derivative of $f(\mathbf{F}^c, L)$ is: $\frac{d^2 f(\mathbf{F}^c, L)}{dt^2} = \sum_k \text{Tr}(\mathbf{Y}_k\mathbf{Y}_k^\dagger + \mathbf{Y}_k\mathbf{Y}_k^\dagger - a_k((\mathbf{G}_k(\mathbf{F}_{-k}^c) + L_{kk}\mathbf{H}_{kk}\mathbf{F}_k^c\mathbf{F}_k^{c\dagger}\mathbf{H}_{kk}^\dagger)^{-1}(\frac{d\mathbf{G}_k(\mathbf{F}_{-k}^c)}{dt} + L_{kk}\mathbf{H}_{kk}\mathbf{Y}_k\mathbf{Y}_k^\dagger \mathbf{H}_{kk}^\dagger)(\frac{d\mathbf{G}_k(\mathbf{F}_{-k}^c)}{dt} + L_{kk}\mathbf{H}_{kk}\mathbf{Y}_k\mathbf{Y}_k^\dagger \mathbf{H}_{kk}^\dagger)^{-1}(\mathbf{G}_k(\mathbf{F}_{-k}^c) + L_{kk}\mathbf{H}_{kk}\mathbf{F}_k^c\mathbf{F}_k^{c\dagger}\mathbf{H}_{kk}^\dagger) + \mathbf{G}_k^{-1}(\mathbf{F}_{-k}^c)(\frac{d\mathbf{G}_k(\mathbf{F}_{-k}^c)}{dt})\mathbf{G}_k^{-1}(\mathbf{F}_{-k}^c)(\frac{d\mathbf{G}_k(\mathbf{F}_{-k}^c)}{dt})))$, where $\frac{d\mathbf{G}_k(\mathbf{F}_{-k}^c)}{dt} = \sum_{j\neq k} L_{kj}\mathbf{H}_{kj}\mathbf{Y}_j\mathbf{Y}_j^\dagger \mathbf{H}_{kj}^\dagger$ does not depend on t. As L becomes sufficiently small, $\frac{d\mathbf{G}_k(\mathbf{F}_{-k}^c)}{dt}$ is proportional to L and $\frac{d\mathbf{G}_k(\mathbf{F}_{-k}^c)}{dt} + L_{kk}\mathbf{H}_{kk}\mathbf{Y}_k\mathbf{Y}_k^\dagger \mathbf{H}_{kk}^\dagger$ is dominated by $L_{kk}\mathbf{H}_{kk}\mathbf{Y}_k\mathbf{Y}_k^\dagger \mathbf{H}_{kk}^\dagger$.

$\mathbf{G}_k^{-1}(\mathbf{F}_{-k}^c)\left(\frac{\mathrm{d}\mathbf{G}_k(\mathbf{F}_{-k}^c)}{\mathrm{d}t}\right)\mathbf{G}_k^{-1}(\mathbf{F}_{-k}^c)\left(\frac{\mathrm{d}\mathbf{G}_k(\mathbf{F}_{-k}^c)}{\mathrm{d}t}\right)$ is proportional to L^2 and hence it has little impact on the first term in the derivative and can be ignored. Therefore,

$$\frac{\mathrm{d}^2 f(\mathbf{F}^c, L)}{\mathrm{d}t^2} \approx \sum_k \mathrm{Tr}\left(\mathbf{Y}_k\mathbf{Y}_k^\dagger + \mathbf{Y}_k\mathbf{Y}_k^\dagger - a_k\left((\mathbf{G}_k(\mathbf{F}_{-k}^c)\right.\right.$$
$$+L_{kk}\mathbf{H}_{kk}\mathbf{F}_k^c\mathbf{F}_k^{c\dagger}\mathbf{H}_{kk}^\dagger)^{-1}\left(\frac{\mathrm{d}\mathbf{G}_k(\mathbf{F}_{-k}^c)}{\mathrm{d}t}+L_{kk}\mathbf{H}_{kk}\mathbf{Y}_k\mathbf{Y}_k^\dagger\mathbf{H}_{kk}^\dagger\right)$$
$$\left(\frac{\mathrm{d}\mathbf{G}_k(\mathbf{F}_{-k}^c)}{\mathrm{d}t}+L_{kk}\mathbf{H}_{kk}\mathbf{Y}_k\mathbf{Y}_k^\dagger\mathbf{H}_{kk}^\dagger\right)^{-1}$$
$$\left.\left.\left(\mathbf{G}_k(\mathbf{F}_{-k}^c)+L_{kk}\mathbf{H}_{kk}\mathbf{F}_k^c\mathbf{F}_k^{c\dagger}\mathbf{H}_{kk}^\dagger\right)\right)\right) \tag{58}$$

Denote $\mathbf{A}_k = (\mathbf{G}_k(\mathbf{F}_{-k}^c) + L_{kk}\mathbf{H}_{kk}\mathbf{F}_k^c\mathbf{F}_k^{c\dagger}\mathbf{H}_{kk}^\dagger)^{-1}$ and $\mathbf{B}_k = \frac{\mathrm{d}\mathbf{G}_k(\mathbf{F}_{-k}^c)}{\mathrm{d}t}+L_{kk}\mathbf{H}_{kk}\mathbf{Y}_k\mathbf{Y}_k^\dagger\mathbf{H}_{kk}^\dagger$. Since $\mathbf{A}_k$ is positive semidefinite, there exists a matrix $\mathbf{X}_k$ such that $\mathbf{A}_k = \mathbf{X}_k\mathbf{X}_k^\dagger$. Thus, from (58), we have $\frac{\mathrm{d}^2 f(\mathbf{F}^c, L)}{\mathrm{d}t^2} \approx \sum_k \mathrm{Tr}(2\mathbf{Y}_k\mathbf{Y}_k^\dagger - a_k\mathbf{A}_k\mathbf{B}_k\mathbf{A}_k\mathbf{B}_k) = \sum_k \mathrm{Tr}(2\mathbf{Y}_k\mathbf{Y}_k^\dagger - a_k\mathbf{X}_k^\dagger\mathbf{B}_k\mathbf{X}_k\mathbf{X}_k^\dagger\mathbf{B}_k\mathbf{X}_k) = \sum_k \mathrm{Tr}(2\mathbf{Y}_k\mathbf{Y}_k^\dagger - a_k(\mathbf{X}_k^\dagger\mathbf{B}_k\mathbf{X}_k)(\mathbf{X}_k^\dagger\mathbf{B}_k\mathbf{X}_k)^\dagger) \geq 0$, for sufficiently small L, where the last equality is due to the fact that $a_k \leq 0$ and $\mathbf{B}_k$ is Hermitian. Therefore, $f(\mathbf{F}, L)$ is convex for sufficiently small L. ∎

Based on Lemma 9, for sufficiently small L, the problem in (23) is convex. Furthermore, since the limiting point $\mathbf{F}(\infty)$ of algorithm 1 is a stationary point of the problem (23), which is also the unique global optimal point of (23).

Appendix G: Proof of Theorem 4

Following the notation of the *Bellman operators* in (31)–(34) in Appendix B, we define two mappings: $T_{\boldsymbol{\chi}}^\dagger(V, \mathbf{F}, \mathbf{U}) = T_{\boldsymbol{\chi}}^\dagger(\theta, V, \mathbf{F}, \mathbf{U}) + \theta = c(\mathbf{Q}, \mathbf{F}) + \sum_{k=1}^K \frac{\partial V(\mathbf{Q})}{\partial Q_k}[R_k(\mathbf{H}, \mathbf{F}, \mathbf{U}) - \mu_k]$, $T_{\boldsymbol{\chi}}(V, \mathbf{F}, \mathbf{U}) = T_{\boldsymbol{\chi}}^\dagger(V, \mathbf{F}, \mathbf{U}) + \tau G_{\boldsymbol{\chi}}(V, \mathbf{F}, \mathbf{U})$.

We calculate the performance under policy $\widetilde{\Omega}$ as follows:

$$\tilde{\theta}\tau = \mathbb{E}^{\widetilde{\Omega}}\left[\mathbb{E}\left[c(\mathbf{Q}, \widetilde{\Omega}(\boldsymbol{\chi}))\tau\Big|\mathbf{Q}\right]\right]$$
$$\stackrel{(a)}{=} \mathbb{E}^{\widetilde{\Omega}}\left[\mathbb{E}\left[c(\mathbf{Q}, \widetilde{\Omega}(\boldsymbol{\chi}))\tau + \sum_{\mathbf{Q}'}\mathrm{Pr}\left[\mathbf{Q}'|(\boldsymbol{\chi}, \widetilde{\Omega}((\boldsymbol{\chi})]\widetilde{V}(\mathbf{Q}') - \widetilde{V}(\mathbf{Q})\Big|\mathbf{Q}\right]\right]$$
$$\stackrel{(b)}{=} \mathbb{E}^{\widetilde{\Omega}}\left[\mathbb{E}\left[c(\mathbf{Q}, \widetilde{\Omega}(\boldsymbol{\chi}))\tau + \sum_{k=1}^K \frac{\partial \widetilde{V}(\mathbf{Q})}{\partial Q_k}\left[R_k(\mathbf{H}, \widetilde{\Omega}(\boldsymbol{\chi})) - \mu_k\right]\tau\Big|\mathbf{Q}\right]\right.$$
$$\left.+\tau^2 G_{\mathbf{Q}}(\widetilde{V}, \widetilde{\Omega}(\mathbf{Q}))\right] \tag{59}$$

where $\mathrm{Pr}\left[\mathbf{Q}'|\boldsymbol{\chi}, \widetilde{\Omega}(\boldsymbol{\chi})\right]$ is the discrete time transition kernel under policy $\widetilde{\Omega}$. (a) is due to $\mathbb{E}^{\widetilde{\Omega}}\left[\sum_{\mathbf{Q}'}\mathbb{E}\left[\mathrm{Pr}\left[\mathbf{Q}'|\boldsymbol{\chi}, \widetilde{\Omega}(\mathbf{Q})\right]|\mathbf{Q}\right]\widetilde{V}(\mathbf{Q}')\right] = \mathbb{E}^{\widetilde{\Omega}}\left[\mathbb{E}^{\widetilde{\Omega}}\left[\widetilde{V}(\mathbf{Q}')|\mathbf{Q}\right]\right] = \mathbb{E}^{\widetilde{\Omega}}\left[\widetilde{V}(\mathbf{Q})\right]$ under the steady state distribution using $\widetilde{\Omega}$, and (b) is due to the Taylor expansion of $\widetilde{V}(\mathbf{Q}')$ at $\widetilde{V}(\mathbf{Q})$.

Let Ω^* be the optimal policy solving the discrete time Bellman equation in (11), then we have

$$\mathbb{E}\left[T_{\boldsymbol{\chi}}(V^*, \Omega^*(\boldsymbol{\chi})|\mathbf{Q}\right] = \theta^*, \quad \forall\mathbf{Q} \tag{60}$$

Furthermore, according to the asymptotic optimality of Algorithm 1 in Lemma 3, we have

$$T_{\boldsymbol{\chi}}^\dagger(\widetilde{V}, \widetilde{\Omega}(\boldsymbol{\chi})) = \min_{\Omega(\mathbf{Q})} T_{\boldsymbol{\chi}}^\dagger(\widetilde{V}, \Omega(\boldsymbol{\chi})), \quad \forall\boldsymbol{\chi} \tag{61}$$

for sufficient small L. Dividing τ on both sizes of (59), we obtain

$$\tilde{\theta} = \mathbb{E}^{\widetilde{\Omega}}\left[\mathbb{E}[T_{\boldsymbol{\chi}}(\widetilde{V}, \widetilde{\Omega}(\boldsymbol{\chi}))|\mathbf{Q}]\right]$$

$$= \mathbb{E}^{\widetilde{\Omega}}\left[\mathbb{E}[T_{\boldsymbol{\chi}}^\dagger(\widetilde{V}, \widetilde{\Omega}(\boldsymbol{\chi})) + \tau G_{\boldsymbol{\chi}}(\widetilde{V}, \widetilde{\Omega}(\boldsymbol{\chi}))|\mathbf{Q}]\right]$$
$$\stackrel{(c)}{\leq} \mathbb{E}^{\widetilde{\Omega}}\left[\mathbb{E}[T_{\boldsymbol{\chi}}^\dagger(\widetilde{V}, \Omega^*(\boldsymbol{\chi})) + \tau G_{\boldsymbol{\chi}}(\widetilde{V}, \widetilde{\Omega}(\boldsymbol{\chi}))|\mathbf{Q}]\right]$$
$$= \mathbb{E}^{\widetilde{\Omega}}\left[\mathbb{E}[T_{\boldsymbol{\chi}}(\widetilde{V}, \Omega^*(\boldsymbol{\chi})) + \tau G_{\boldsymbol{\chi}}(\widetilde{V}, \widetilde{\Omega}(\boldsymbol{\chi})) - \tau G_{\boldsymbol{\chi}}(\widetilde{V}, \Omega^*(\boldsymbol{\chi}))|\mathbf{Q}]\right]$$
$$\stackrel{(d)}{=} \mathbb{E}^{\widetilde{\Omega}}\left[\mathbb{E}[T_{\boldsymbol{\chi}}(\widetilde{V}, \Omega^*(\boldsymbol{\chi})) - T_{\boldsymbol{\chi}}(V^*, \Omega^*(\boldsymbol{\chi})) + \theta^*\right.$$
$$\left.+ \tau G_{\boldsymbol{\chi}}(\widetilde{V}, \widetilde{\Omega}(\boldsymbol{\chi})) - \tau G_{\boldsymbol{\chi}}(\widetilde{V}, \Omega^*(\boldsymbol{\chi}))|\mathbf{Q}]\right] \tag{62}$$

where (c) is due to (61) and (d) is due to (60). For any given $\boldsymbol{\chi}$, since $G_{\boldsymbol{\chi}}$ is a smooth and bounded function, we have $\tau G_{\boldsymbol{\chi}}(\widetilde{V}, \widetilde{\Omega}(\boldsymbol{\chi})) - \tau G_{\boldsymbol{\chi}}(\widetilde{V}, \Omega^*(\boldsymbol{\chi})) = \mathcal{O}(\tau)$. Therefore, from (62), we have $\tilde{\theta} - \theta^* \leq \mathbb{E}^{\widetilde{\Omega}}\left[\mathbb{E}[T_{\boldsymbol{\chi}}(\widetilde{V}, \Omega^*(\boldsymbol{\chi})) - T_{\boldsymbol{\chi}}(V^*, \Omega^*(\boldsymbol{\chi}))|\mathbf{Q}] + \mathcal{O}(\tau) \stackrel{(e)}{\leq} \alpha\|V^* - \widetilde{V}\|_\infty^\omega + \mathcal{O}(\tau) \stackrel{(f)}{\leq} o(1) + \mathcal{O}(L) + \mathcal{O}(\tau) = o(1) + \mathcal{O}(L)$, where $\alpha > 0$ is some constant, $V^* = \{V^*(\mathbf{Q}) : \forall\mathbf{Q}\}$ and $\widehat{V} = \{\widetilde{V}(\mathbf{Q}) : \forall\mathbf{Q}\}$. (e) holds under some sup-norm $\|\cdot\|_\infty^\omega$, which is due to the Lipchitz continuity of the operator $T_{\boldsymbol{\chi}}$ [10] and (f) is due to $V(\mathbf{Q}) - \widetilde{V}(\mathbf{Q}) = o(1) + \mathcal{O}(L)$.

References

[1] V. R. Cadambe and S. A. Jafar, "Interference alignment and degrees of freedom of the K-user interference channel," *IEEE Trans. Inf. Theory*, vol. 54, no. 8, pp. 3425–3441, Aug. 2008.

[2] B. Norsat-Makouei, J. G. Andrews, and R. W. Heath, "MIMO interference alignment over correlated channels with imperfect CSI," *IEEE Trans. Signal Process.*, vol. 59, no. 6, pp. 2783–2794, June 2011.

[3] S. Serbetli and A. Yener, "Transceiver optimization for multiuser MIMO systems," *IEEE Trans. Signal Process.*, vol. 52, no. 1, pp. 214–226, Jan. 2004.

[4] M. Schubert, H. Boche, "Iterative multiuser uplink and downlink beamforming under SINR constraints," *IEEE Trans. Signal Process.*, vol. 53, no. 7, pp. 2324–2334, 2005.

[5] E. Bjornson, R. Zakhour, D. Gesbert, and B. Ottersten, "Cooperative multicell precoding: Rate region characterization and distributed strategies with instantaneous and statistical CSI," *IEEE Trans. Signal Process.*, vol. 58, no. 8, pp. 4298–4310, Aug. 2010.

[6] D. H. N. Nguyen and T. Le-Ngoc, "Multiuser downlink beamforming in multicell wireless systems: A game theoretical approach," *IEEE Trans. Signal Process.*, vol. 59, no. 7, pp. 3326–3338, 2011.

[7] S. Marano, V. Matta, P. Willett, and L. Tong, "Cross-layer design of sequential detectors in sensor networks," *IEEE Trans. Signal Process.*, vol. 54, no. 11, pp. 4105–4117, Nov. 2011.

[8] A. Ribeiro, "Ergodic stochastic optimization algorithms for wireless communication and networking," *IEEE Trans. Signal Process.*, vol. 58, no. 12, pp. 6369–6386, Sep. 2010.

[9] X. Cao, *Stochastic Learning and Optimization: A Sensitivity-Based Approach*. Springer, 2008.

[10] D. P. Bertsekas, *Dynamic Programming and Optimal Control*, 3rd ed. Massachusetts: Athena Scientific, 2007.

[11] C. Comaniciu and H. V. Poor, "Jointly optimal power and admission control for delay sensitive traffic in CDMA networks with LMMSE receivers," *IEEE Trans. Signal Process.*, vol. 51, no. 8, pp. 2031–2042, Sep. 2003.

[12] R. Berry and R. G. Gallager, "Communication over fading channels with delay constraints," *IEEE Trans. Inform. Theory*, vol. 48, no. 5, pp. 1135–1149, 2002.

[13] M. J. Neely, "Energy optimal control for time varying wireless networks," *IEEE Trans. Inf. Theory*, vol. 52, no. 7, pp. 2915–2934, Jul. 2006.

[14] M. J. Neely, E. Modiano, and C. E. Rohrs, "Dynamic power allocation and routing for time varying wireless networks," *IEEE J. Sel. Areas Commun.*, vol. 23, no. 1, pp. 89–103, Jan. 2005.

[15] Y. Zhang, F. Fu, and M. van der Schaar, "On-line learning and optimization for wireless video transmission," *IEEE Trans. Signal Process.*, vol. 58, no. 6, pp. 3108–3124, 2010.

[16] J. W. Huang, H. Mansour, and V. Krishnamurthy, "A dynamical games approach to transmission-rate adaptation in multimedia WLAN," *IEEE Trans. Signal Process.*, vol. 58, no. 7, pp. 3635–3646, Sep. 2010.

[17] Q. Shi, M. Razaviyayn. Z.-Q. Luo, and C. He, "An iteratively weighted MMSE approach to distributed sum-utility maximization for a MIMO interfering broadcast channel," *IEEE Trans. Signal Process.*, vol. 59, no. 9, pp. 331–4340, 2011.

[18] D. Astély, E. Dahlman, A. Furuskar, Y. Jading, M. Lindstrom, and S. Parkvall, "LTE: the evolution of mobile broadband," *IEEE Commun. Mag.*, vol. 47, no. 4, pp. 44–51, 2009.

[19] R. Zhang, C. C. Chai, and Y.-C. Liang, "Joint beamforming and power control for multiantenna relay broadcast channel with QoS constraints," *IEEE Trans. Signal Process.*, vol. 57, no. 2, pp. 726–737, 2009.

[20] F. Verdicchio, A. Munteanu, A. I. Gavrilescu, J. Cornelis, and P. Schelkens, "Embedded multiple description coding of video," *IEEE Trans. Image Process.*, vol. 15, no. 10, pp. 3114–3130, 2006.

[21] Z. Han, Z. Ji, and K. J. R. Liu, "Non-cooperative resource competition game by virtual referee in multi-cell OFDMA networks," *IEEE J. Sel. Areas Commun.*, vol. 25, pp. 1079–1090, Aug. 2007.

[22] R. Samano-Robles, M. Ghogho, and D. C. McLernon, "Wireless networks with retransmission diversity and carrier-sense multiple access," *IEEE Trans. Signal Process.*, vol. 57, no. 9, pp. 3722–3726, 2009.

[23] D. Qiao, S. Choi, and K. G. Shin, "Interference analysis and transmit power control in IEEE 802.11 a/h wireless LANs," *IEEE/ACM Trans. Netw.*, vol. 15, no. 5, pp. 1007–1020, 2007.

[24] Zcomax Technologies, "IEEE 802.11g (54Mbps) mini PCI Wireless LAN Module," XG-623HP mPCI WLAN Module datasheet, Jan. 2007.

[25] Y. Cui, V. K. N. Lau, R. Wang, H. Huang, and S. Zhang, "A survey on delay-aware resource control for wireless systems - large deviation theory, stochastic Lyapunov drift and distributed stochastic Learning," *IEEE Trans. Inf. Theory*, vol. 58, no. 3, pp. 1677–1701, Mar. 2012.

[26] Q. H. Spencer, A. L. Swindlehurst, and M. Haardt, "Zero-forcing methods for downlink spatial multiplexing in multiuser MIMO channels," *IEEE Trans. Signal Process.*, vol. 52, no. 2, pp. 461–471, 2004.

[27] S. Harsha, A. Kumar, and V. Sharma, "An analytical model for performance evaluation of multimedia applications over EDCA in an IEEE 802.11 e WLAN," *J. Wireless Netw.*, vol. 16, pp. 367385, Feb. 2010.

[28] G. Arslan, M. F. Demirkol, and Y. Song, "Equilibrium efficiency improvement in MIMO interference systems: A decentralized stream control approach," *IEEE Trans. Wireless Commun.*, vol. 6, no. 8, pp. 2984–2993, Aug. 2007.

[29] D. Tse and P. Viswanath, *Fundamentals of Wireless Communication*. Cambridge Univ. Press, 2005.

[30] E. Telatar, "Capacity of multi-antenna Gaussian channels", *European transactions on telecommunications*, Wiley Online Library, vol. 10, no. 6, pp. 585–595, 1999.

[31] J. F. Bonnans and A. Shapiro, "Optimization Problems with Perturbations: A Guided Tour," *SIAM Reviews*, vol. 40, no. 2, pp. 228–264, June 1998.

[32] A. D. Polyanin, V. F. Zaitsev, and A. Moussiaux, *Handbook of First Order Partial Differential Equations*, 2nd ed. Taylor & Francis, 2002.

[33] S. Boyd and L. Vandenberghe, *Convex Optimization*. Cambridge, U.K.: Cambridge Univ. Press, 2004.